Viscoelasticity and Rate-Dependent Continuum Damage Models

M. Cervera

Monograph CIMNE Nº-79, September 2003

Viscoelasticity and Rate-Dependent Continuum Damage Models

M. Cervera

Monograph CIMNE Nº-79, September 2003

INTERNATIONAL CENTER FOR NUMERICAL METHODS IN ENGINEERING
Gran Capitán s/n, 08034 Barcelona, Spain

INTERNACIONAL CENTER FOR NUMERICAL METHODS IN ENGINEERING
Edificio C1, Campus Norte UPC
Gran Capitán s/n
08034 Barcelona, Spain
www.cimne.upc.es

First edition: September 2003

VISCOELASTICITY AND RATE-DEPENDENT CONTINUUM DAMAGE MODELS
Monograph CIMNE M79

ISBN: 84-95999-37-4

Depósito legal: B-40324-2003

Contents

1 VISCOELASTICITY

Constitutive model

In classical viscoelasticity, the mechanical behaviour is characterized by the relaxation function or the compliance function and the constitutive relationships are formulated in the form of Volterra integral equations [Bazant 1988]. This approach is clearly unsuitable for numerical computations because of its memory and CPU time requirements.

However, it is possible to expand any relaxation function into a Dirichlet series, and retain only a finite number of terms. This achieves a double goal: first, the constitutive laws for the viscoelastic material can be written in terms of a finite number of internal variables, and only these need to be stored from one time step to the next, thus providing huge computational advantages compared to the hereditary integral equations; and secondly, the resulting rheological model can be interpreted as a generalized Maxwell chain, where a number of springs and dashpots are arranged in parallel. Alternatively, the compliance function of concrete can be considered and expanded in a Dirichlet series. This leads to a generalized Kelvin chain with a series arrangement. Although both approaches are completely equivalent (if a large enough number of terms is considered in the Dirichlet series), the first one leads to first order differential equations to be solved for the evolution of the internal variables, while the second approach leads to second order differential equations [Carol and Bazant 1993]. Therefore, the Maxwell chain model is preferred here.

Figure 1 shows a schematic representation of the rheological model used, in the form of a Maxwell chain. The elastic moduli, E^i, and the dashpot viscosities, η^i, of the $i = 0, 1, ..., N$ Maxwell elements of the chain are the material parameters. It is also helpful to consider the elastic moduli, E^i, and the relaxation

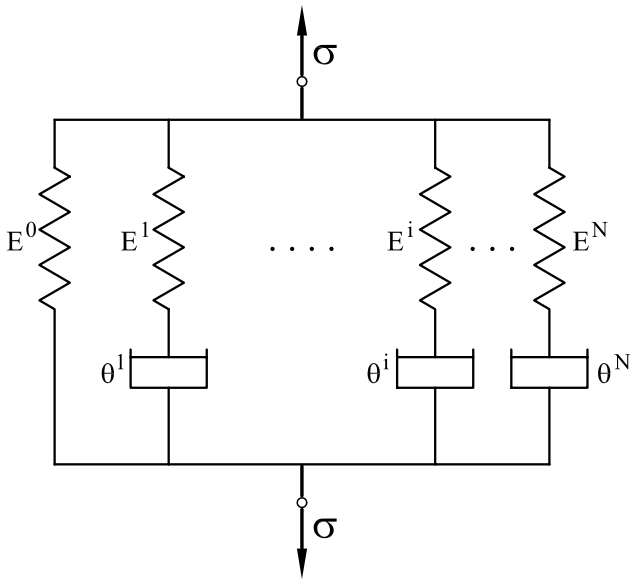

Figure 1 Maxwell chain

times of the dashpots, defined as $\vartheta^i = \eta^i/E^i$, as an alternative characterization of the chain.

It is convenient to take $\vartheta^0 = \infty$ in the series expansion, so that E^0 can be considered as the *asymptotic* elastic modulus. Note that $E = \sum_{i=0}^{N} E^i$ is the *instantaneous* elastic modulus of the material.

It is also useful to define the participation ratio for each element in the chain, ξ^i,as the ratio between its own elastic modulus and that of the chain: $\xi^i = E^i/E$. Note that $\sum_{i=0}^{N} \xi^i = 1$.

The total stress sustained by the Maxwell chain is evaluated as

$$\boldsymbol{\sigma} = \sum_{i=0}^{N} \boldsymbol{\sigma}^i \tag{1.1}$$

Choosing the stress in each Maxwell element of the chain, $\boldsymbol{\sigma}^i$, as internal variables, the first order differential equations governing the evolution of these variables are

$$\dot{\boldsymbol{\sigma}}^i + \frac{\boldsymbol{\sigma}^i}{\vartheta^i} = \xi^i \, \mathbf{D} \, \dot{\boldsymbol{\varepsilon}} \quad \text{for} \quad i = 0, 1, ..., N \tag{1.2}$$

where tensor entities are used as the multidimensional counterparts of the scalar ones used for uniaxial models; $\boldsymbol{\varepsilon}$ is the total strain tensor and $\mathbf{D}$ is the fourth-order elastic constitutive tensor.

It is possible to select the viscous strains in each Maxwell element, $\boldsymbol{\varepsilon}^i$, rather than the stress, $\boldsymbol{\sigma}^i$, as internal variables.

The relationship between them is

$$\boldsymbol{\sigma}^i \,=\, \xi^i \mathbf{D} : (\boldsymbol{\varepsilon} - \boldsymbol{\varepsilon}^i) \tag{1.3}$$

Substitution of Eq. (1.3) into Eq. (1.2) leads to the obtention of the evolution law for the viscous strains

$$\dot{\boldsymbol{\varepsilon}}^i \,=\, \frac{1}{\vartheta^i}\,(\boldsymbol{\varepsilon} - \boldsymbol{\varepsilon}^i) \qquad \text{for} \quad i \,=\, 0, 1, ..., N \tag{1.4}$$

Thermodynamic Framework

Let us define the elastic free energy associated to each element in the Maxwell chain in the form

$$W_e^i \;=\; W_e^i(\boldsymbol{\varepsilon}_e^i) \;=\; \frac{1}{2}\,\boldsymbol{\sigma}^i : (\xi^i\,\mathbf{D})^{-1} : \boldsymbol{\sigma}^i \tag{1.5a}$$

$$\;=\; \frac{1}{2}\,\boldsymbol{\varepsilon}_e^i : (\xi^i\,\mathbf{D}) : \boldsymbol{\varepsilon}_e^i \tag{1.5b}$$

where the elastic strain tensor is defined as $\boldsymbol{\varepsilon}_e^i = \boldsymbol{\varepsilon} - \boldsymbol{\varepsilon}^i$, for each element. The total elastic free energy associated to the Maxwell chain is obtained by adding the contributions of the elements

$$W_e \,=\, W_e(\boldsymbol{\varepsilon}_e^i) \,=\, \sum_{i=0}^{N} W_e^i(\boldsymbol{\varepsilon}_e^i) \tag{1.6}$$

Using Coleman's method, the total stress can be obtained as

$$\boldsymbol{\sigma} \,=\, \partial_{\boldsymbol{\varepsilon}} W_e \,=\, \sum_{i=0}^{N} \partial_{\boldsymbol{\varepsilon}} W_e^i \,=\, \sum_{i=0}^{N} \xi^i \mathbf{D} : \boldsymbol{\varepsilon}_e^i \,=\, \sum_{i=0}^{N} \boldsymbol{\sigma}^i \tag{1.7}$$

Note that the introduced viscous strains $\boldsymbol{\varepsilon}^i$ are the thermodynamic forces conjugated to the stresses in the chain elements $\boldsymbol{\sigma}^i$ ($\boldsymbol{\sigma}^i = -\partial_{\boldsymbol{\varepsilon}^i} W_e$). Also, the mechanical dissipation for the Maxwell chain can be computed as

$$\dot{D}_{\text{mech}} \,=\, \sum_{i=0}^{N} \frac{2}{\vartheta^i}\, W_e^i \;\geq\; 0 \tag{1.8}$$

The evolution law for the viscous strains is

$$\dot{\boldsymbol{\varepsilon}}^i = \frac{1}{\vartheta^i}\left(\boldsymbol{\varepsilon} - \boldsymbol{\varepsilon}^i\right) \qquad \text{for} \quad i = 0, 1, ..., N \tag{1.9}$$

whose solution in time is of the form [Cervera et al. 1992]:

$$\boldsymbol{\varepsilon}^i = \frac{1}{\vartheta^i}\int_{-\infty}^{t} e^{-\frac{t-s}{\vartheta^i}}\boldsymbol{\varepsilon}(s)\,ds \tag{1.10}$$

This can be expressed, for time $t_{n+1} = t_n + \Delta t$ as

$$\begin{aligned}
\boldsymbol{\varepsilon}^i(t_{n+1}) &= \frac{1}{\vartheta^i}\int_{-\infty}^{t_{n+1}} e^{-\frac{(t_{n+1})-s}{\vartheta^i}}\boldsymbol{\varepsilon}(s)\,ds && \text{(1.11a)}\\
&= \frac{1}{\vartheta^i}\int_{-\infty}^{t_n} e^{-\frac{(t_n-s)}{\vartheta^i}} e^{-\frac{\Delta t}{\vartheta^i}}\boldsymbol{\varepsilon}(s)\,ds + && \text{(1.11b)}\\
&\qquad + \frac{1}{\vartheta^i}\int_{-\infty}^{t_{n+1}} e^{-\frac{(t_{n+1})-s}{\vartheta^i}}\boldsymbol{\varepsilon}(s)\,ds\\
&= \boldsymbol{\varepsilon}^i(t_n)\, e^{-\frac{\Delta t}{\vartheta^i}} + \Delta\boldsymbol{\varepsilon}^i && \text{(1.11c)}
\end{aligned}$$

with the increment of viscous strain equal to the second integral term

$$\Delta\boldsymbol{\varepsilon}^i = \frac{1}{\vartheta^i}\int_{-\infty}^{t_{n+1}} e^{-\frac{(t_{n+1})-s}{\vartheta^i}}\boldsymbol{\varepsilon}(s)\,ds \tag{1.12}$$

The numerical integration of Eq. (1.12) can be performed by different methods. Here, we will assume that the strain is approximately constant during the interval $[t_n, t_{n+1}]$ and equal to the value at time t^*, (with $t^* = t_n + \alpha\Delta t$, $0 \le \alpha \le 1$). Then, Eq. (1.12) can be evaluated as

$$\begin{aligned}
\Delta\boldsymbol{\varepsilon}^i &= \frac{1}{\vartheta^i}\boldsymbol{\varepsilon}(t^*)\int_{-\infty}^{t_{n+1}} e^{-\frac{t_{n+1}}{\vartheta^i}} e^{\frac{s}{\vartheta^i}}\,ds && \text{(1.13a)}\\
&= \boldsymbol{\varepsilon}(t^*)\, e^{-\frac{t_{n+1}}{\vartheta^i}}\left[e^{\frac{s}{\vartheta^i}}\right]_{t_n}^{t_{n+1}} && \text{(1.13b)}\\
&= \boldsymbol{\varepsilon}(t^*)\left(1 - e^{-\frac{\Delta t}{\vartheta^i}}\right) && \text{(1.13c)}
\end{aligned}$$

and, therefore, Eq. (1.11c) is

$$\boldsymbol{\varepsilon}^i(t_{n+1}) = \boldsymbol{\varepsilon}^i(t_n)\, e^{-\frac{\Delta t}{\vartheta^i}} + \boldsymbol{\varepsilon}(t^*)\left(1 - e^{-\frac{\Delta t}{\vartheta^i}}\right) \tag{1.14}$$

Taking $\alpha = 0$, then $t^* = t_n$ and it is necessary to store $\boldsymbol{\varepsilon}(t_n)$ to integrate the viscous strains. It is, therefore, computationally

more efficient to use $\alpha = 1$, $t^* = t_{n+1}$, and then Eq. (1.11c) reduces to

$$\boldsymbol{\varepsilon}^i(t_{n+1}) = \boldsymbol{\varepsilon}^i(t_n)\, e^{-\frac{\Delta t}{\vartheta^i}} + \boldsymbol{\varepsilon}(t_{n+1}) \left(1 - e^{-\frac{\Delta t}{\vartheta^i}}\right) \tag{1.15}$$

It must be remarked that this integration method is *unconditionally stable*.

For small time steps, $\frac{\Delta t}{\vartheta^i} << 1$, $e^{-\frac{\Delta t}{\vartheta^i}} \simeq 1 - \frac{\Delta t}{\vartheta^i}$, and Eq. (1.15) can be rewritten as

$$\boldsymbol{\varepsilon}^i(t_{n+1}) = \boldsymbol{\varepsilon}^i(t_n) \; + \frac{\Delta t}{\vartheta^i} \left[\boldsymbol{\varepsilon}(t_{n+1}) - \boldsymbol{\varepsilon}^i(t_n)\right] \tag{1.16}$$

which obviously corresponds to using a backward Euler scheme on Eq. (1.9).

Tangent operator

The tangent operator consistent with the numerical integration scheme proposed can be obtained by differentiating Eq. (1.1) with respect to time, substituting Eq. (1.3), and differentiating the integration scheme Eq. (1.15), to obtain:

$$\begin{aligned}
\dot{\boldsymbol{\sigma}} &= \sum_{i=0}^{N} \dot{\boldsymbol{\sigma}}^i && \text{(1.17a)} \\
&= \sum_{i=0}^{N} \xi^i \mathbf{D} : (\dot{\boldsymbol{\varepsilon}} - \dot{\boldsymbol{\varepsilon}}^i) && \text{(1.17b)} \\
&= \left[\sum_{i=0}^{N} \xi^i e^{-\frac{\Delta t}{\vartheta^i}}\right] \mathbf{D} : \dot{\boldsymbol{\varepsilon}} && \text{(1.17c)} \\
&= \mathbf{D}^{\text{visc}} : \dot{\boldsymbol{\varepsilon}} && \text{(1.17d)}
\end{aligned}$$

Therefore, the viscoelastic tangent operator is

$$\mathbf{D}^{\text{visc}} = \left[\sum_{i=0}^{N} \xi^i e^{-\frac{\Delta t}{\vartheta^i}}\right] \mathbf{D} \tag{1.18}$$

Note that for very small time steps, $\frac{\Delta t}{\vartheta^i} \to 0$, the viscoelastic operator is purely elastic, $\mathbf{D}^{\text{visc}} \to \mathbf{D}$. Also, for large time steps, $\frac{\Delta t}{\vartheta^i} >> 1$, the response tends to be asymptotic, $\mathbf{D}^{\text{visc}} \to (E^0/E)\, \mathbf{D}$.

Note that for $\frac{\Delta t}{\vartheta^i} << 1$, $e^{-\frac{\Delta t}{\vartheta^i}} \simeq 1 - \frac{\Delta t}{\vartheta^i}$, and the viscoelastic tangent operator for a backward Euler scheme is:

$$\mathbf{D}^{\text{visc}} = \left[\sum_{i=0}^{N} \xi^i \left(1 - \frac{\Delta t}{\vartheta^i}\right)\right] \mathbf{D} \tag{1.19}$$

Numerical examples

In order to verify the performance of the constitutive viscoelastic model described above, some numerical examples are presented.

These examples focus on the influence of the parameters defining the model on the obtained behaviour. The parameters needed to define the viscoelastic model are summarized in Table 1.1. In this Table, reference to the different material properties is made both in the notation used in the text and with the names of the variables that the finite element program COMET [Cervera et al. 2002] uses to denote the corresponding parameters.

Name	**Text**	**Variable**
Young's modulus	E	`YOUNG`
Poisson's ratio	ν	`POISS`
Number of Maxwell chains	N	`NMAXW`
Elasticity modulus ratio for chain i	ξ^i	`ELASi`
Relaxation time for chain i	ϑ^i	`RETAi`

Table 1.1 Parameters used in the model

To conduct the desired tests on the numerical integration of the constitutive model a finite element model must be defined, together with the appropriate boundary and loading conditions. To this end, a FE mesh consisting of a single four-noded element of 1×1 m in the $x - y$ plane, simply (isostatically) supported is used. Plane strain conditions are assumed in the z-direction. The element is loaded in x-direction by imposing a prescribed displacement that follows the cyclic time history shown in Figure 2. A constant time step size of $\Delta t = 10$ s was used to perform the analyses.

Two different cases are defined to study the influence of the number of Maxwell chains and their material properties. The values used in the models are showed in Table 1.2. All units

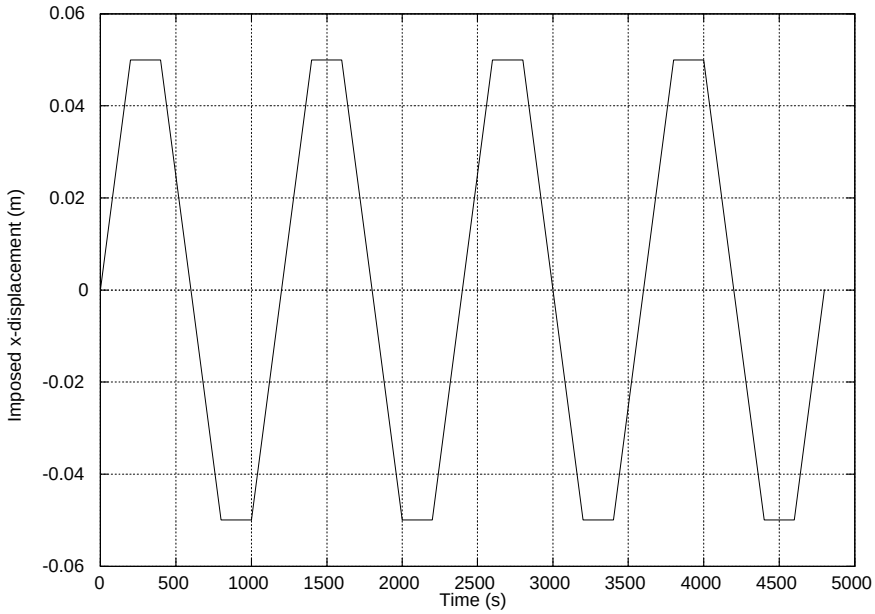

Figure 2 Cyclic load

are in the SI system. Note that Case 1 consists of 2 elements, with $\xi^0 = \xi^1 = 0.5$ and $\vartheta^0 = \infty$, $\vartheta^1 = 100$. Case 2 consists of 3 elements, with $\xi^0 = \xi^1 = \xi^2 = 0.33$ and $\vartheta^0 = \infty$, $\vartheta^1 = 100$, $\vartheta^2 = 1\,000$.

Variable	**Case 1**	**Case 2**
YOUNG	100 000	100 000
POISS	0.3	0.3
NMAXW	1	2
ELAS1	0.5	0.33
RETA1	100	100
ELAS2	–	0.33
RETA2	–	1 000

Table 1.2 Values of material properties

Results for Case 1 are shown in Figures 3 and 4. Figure 3 shows the stress evolution in time, compared with a purely elastic behaviour. Figure 4 shows the corresponding stress *versus* strain curve. Figures 5 and 6 show the corresponding results for Case 2.

In both cases, the influence of the viscous terms are evident, particularly in the relaxation of stresses that takes place under sustained strain. These effects are slightly larger for Case 2. Note also how the solution tends to a steady state cycle after 1 and 2 cycles, respectively.

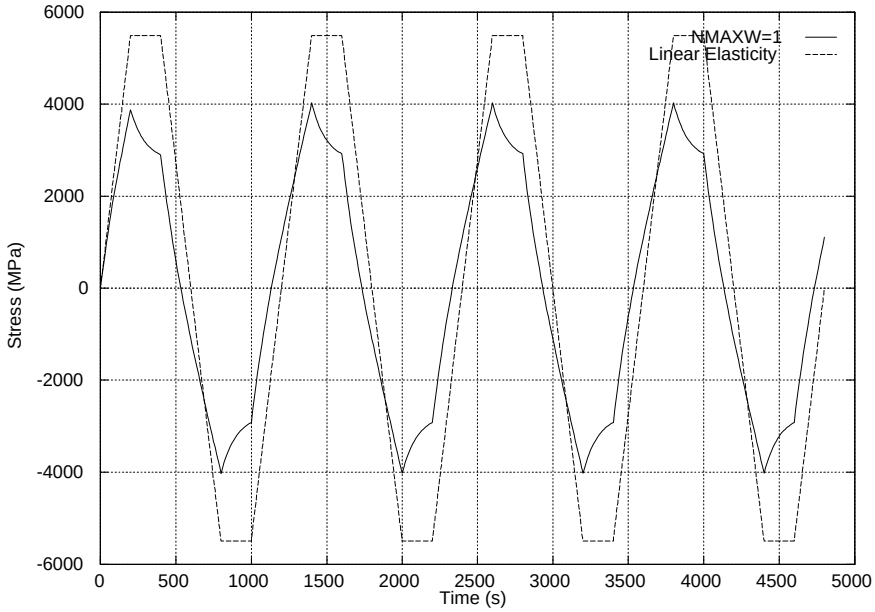

Figure 3 Stress vs. Time for Case 1

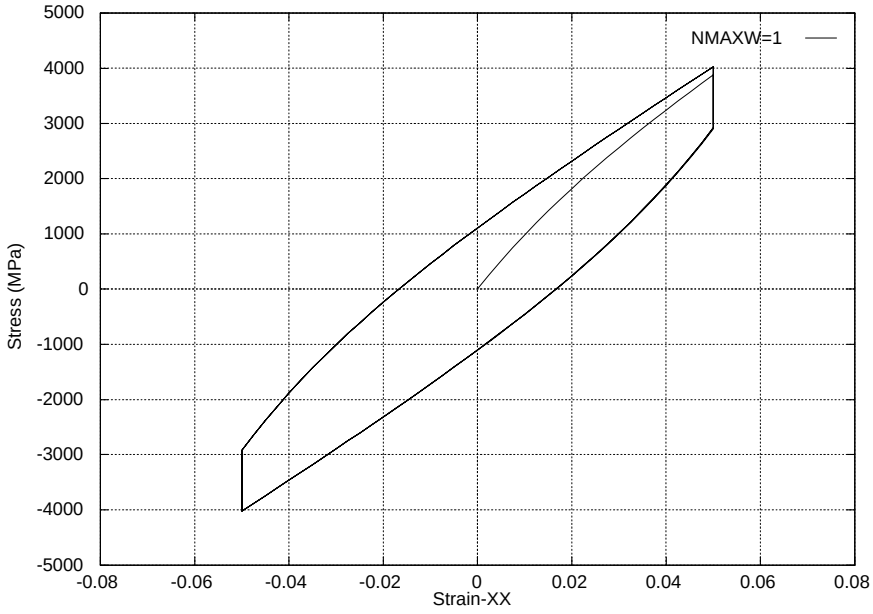

Figure 4 Stress vs. Strain for Case 1

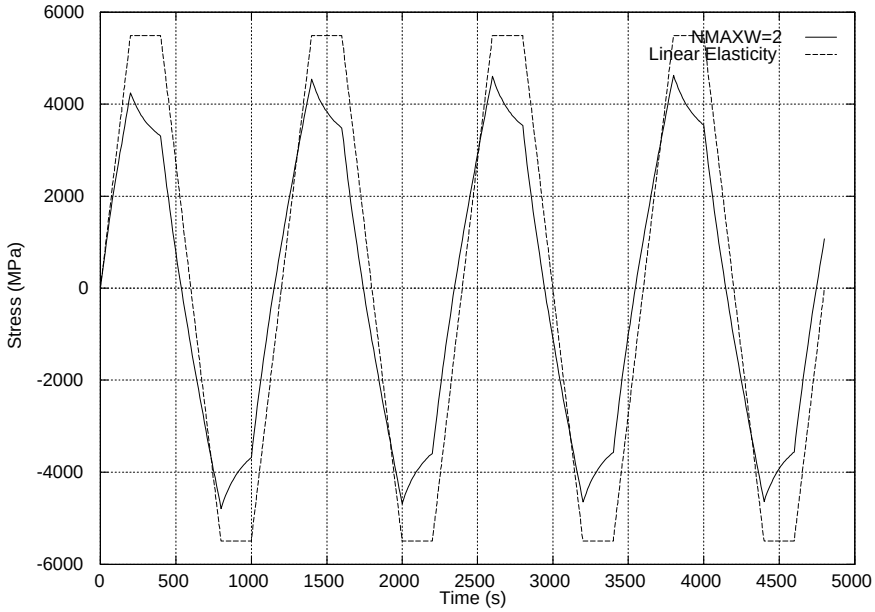

Figure 5 Stress vs. Time for Case 2

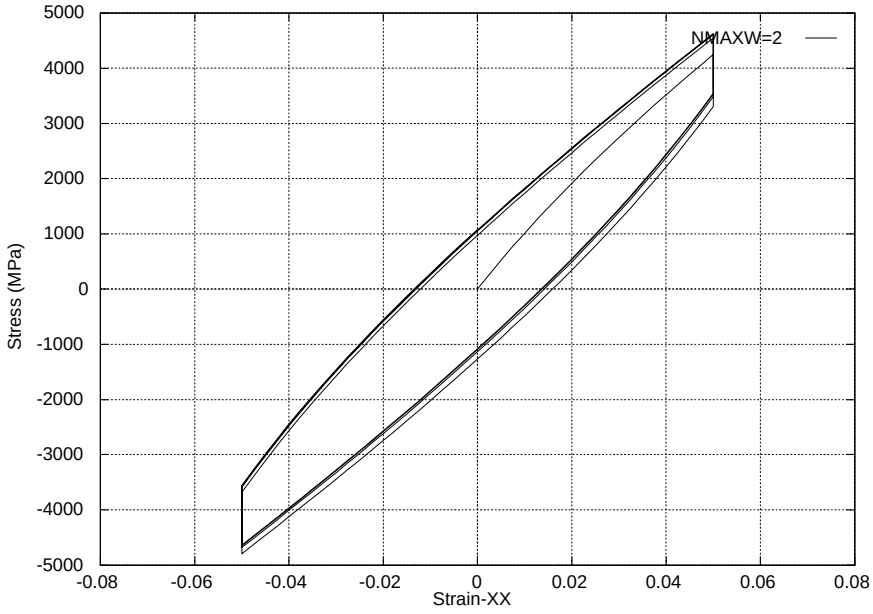

Figure 6 Stress vs. Strain for Case 2

2 ISOTROPIC DAMAGE

Constitutive model

Introduction

The mechanical behaviour of many materials is complex and highly nonlinear, even for moderate stress levels. The available literature on material modelling includes models based on the theories of hypoelasticity, hyperelasticity, plasticity, fracture mechanics, plastic–fracture, or continuum damage, to name only some of the more popular ones. The present work will make use of an *isotropic continuum damage model* to characterize the mechanical behaviour of materials. The Continuum Damage Theory was firstly introduced by Kachanov (1958) in the context of creep–related problems, but it has afterwards been accepted as a valid alternative to deal with complex material behaviour. It is nowadays used for materials so different as metals, ceramics, rock and concrete, and within a wide range of applications (creep, fatigue, progressive failure, etc.). The reason for its popularity is as much the intrinsic simplicity and versatility of the approach, as well as its consistency, based on the theory of thermodynamics of irreversible processes.

The present work will make use of a *continuum damage model* to characterize this type of mechanical behaviour. In particular, we will formulate an *isotropic damage model*, with only one scalar internal variable to monitor the local damage (Simó and Ju 1987, Cervera et al 1995, 1996). This will provide a simple constitutive model which, nevertheless, is able to reproduce overall non–linear behaviour including stiffness degradation, strain–softening response and rate dependency. Furthermore, the model can be implemented in a strain–driven form which leads to an almost closed–form algorithm to integrate the stress tensor in time. This is a most valuable feature for a model intended to be used in large scale computations.

Effective Stresses

The Continuum Damage Mechanics Theory (CDMT) is based on the definition of the effective stress concept, which is introduced in connection with the hypothesis of strain equivalence [Lemaitre and Chaboche 1978]: the strain associated with a damaged state under the applied stress σ is equivalent to the strain associated with its undamaged state under the effective stress $\bar{\sigma}$. In the present work the (second order) effective stress tensor $\overline{\boldsymbol{\sigma}}$ will assume the following hyper-elastic form:

$$\overline{\boldsymbol{\sigma}} = \mathbf{D} : \boldsymbol{\varepsilon} \tag{2.1}$$

where $\boldsymbol{\varepsilon}$ is the (second order) strain tensor, $\mathbf{D}$ is the usual (fourth order) linear–elastic constitutive tensor and (:) denotes the tensorial product contracted on two indices.

Constitutive Equation

The constitutive equation for the damage model is obtained using Coleman's method as:

$$\boldsymbol{\sigma} = \ (1 - d)\, \overline{\boldsymbol{\sigma}} \tag{2.2}$$

where we have introduced one internal-like variable, d, the damage index, whose definition and evolution in terms of the real internal variable will be given later.

Characterization of Damage

In order to clearly define concepts such as loading, unloading, or reloading for general 3D stress states, a scalar positive quantity, termed as *normalized equivalent stress*, will be defined. This will permit the comparison of different 3D stress states. With such a definition, distinct tridimensional stress states can be mapped to a single *normalized equivalent 1D stress test*, which makes their quantitative comparison possible [Simó and Ju 1987a].

In the present work the *normalized equivalent stress* will assume the following form:

$$\tau \ = \ \left[\left(\frac{\overline{\boldsymbol{\sigma}}}{f_e} \right) : \mathbf{C} : \left(\frac{\overline{\boldsymbol{\sigma}}}{f_e} \right) \right]^{1/2} \ = \ \frac{1}{f_e} \left[\overline{\boldsymbol{\sigma}} : \mathbf{C} : \overline{\boldsymbol{\sigma}} \right]^{1/2} \tag{2.3}$$

where the non-dimensional fourth order metric tensor $\mathbf{C}$ has been introduced. The role of this tensor is to define the shape of the damage bounding surface in a normalized effective stress space, as it will be explained below.

The normalizing factor f_e represents the value of the uniaxial stress that defines the onset of damage under uniaxial tension and compression, assumed to be the same.

With the above definitions for the equivalent effective stress, the damage criterion, g is introduced:

$$g(\tau, r) = \tau - r \leq 0 \tag{2.4}$$

Variable r is a normalized internal strain-like variable which can be interpreted as the current damage threshold, in the sense that its value controls the size of the (monotonically) expanding damage surface. Due to its normalized nature, the initial value is unitary, $r_0 = 1$.

This means that the damage criterion is defined in a normalized effective stress space (or in a normalized strain space). In fact, the shape of the damage criterion is defined by the metric tensor $\mathbf{C}$. This tensor must be isotropic and positive definite, in the form:

$$\mathbf{C} = (1+\gamma)\,\mathbf{I} - \gamma\,\mathbf{1}\otimes\mathbf{1} \qquad \text{with} \qquad 0 \leq \gamma < 1 \tag{2.5}$$

where $\mathbf{I}$ is the fourth order unit tensor, $\mathbf{1}$ is the second order unit tensor and γ is a parameter related to the equibiaxial strength. Calling ρ to the ratio between the biaxial and uniaxial strengths, it is

$$\gamma = 1 - \frac{1}{2\,(\rho)^2} \tag{2.6}$$

Figures 1 and 2 show 2D representations of the damage criteria for two possible selections of this tensor:

(a) $\gamma = 0$, $\mathbf{C} = \mathbf{I}$ represents a rounded Rankine-type of criterion with $\rho = 1/\sqrt{2} = 0.707$;

(b) $\gamma = \nu$, $\mathbf{C} = \overline{\mathbf{D}}^{-1} = (\mathbf{D}/E)^{-1}$ represents a criterion related to the (normalized) elastic free energy, leading to $\rho = 0.767$.

In this work, we will use option (b). Note that options (a) and (b) are identical if the effect of Poisson's ratio is disregarded.

The evolution (expansion) of the damage bounding surface in the normalized space for loading, unloading and reloading conditions is controlled by the Kuhn-Tucker relations and the damage consistency condition, which are

$$\dot{r} \geq 0 \qquad g \leq 0 \qquad \dot{r}\,g = 0 \tag{2.7a}$$

$$\dot{r}\,\dot{g} = 0 \tag{2.7b}$$

leading, in view of Eq. (2.4), to the loading condition

$$\dot{r} = \dot{\tau} \tag{2.8}$$

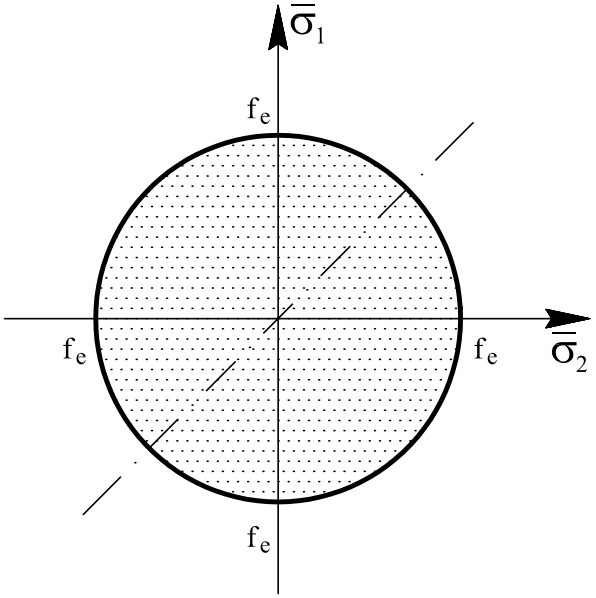

Figure 1 Rankine type of damage criterion

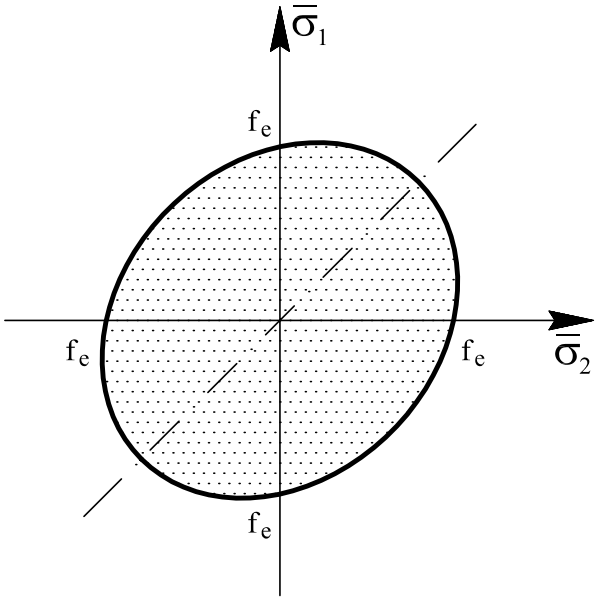

Figure 2 Energy norm damage criterion

This, in turn, leads to the explicit definition of the current values of the internal variable r in the form

$$r = \max\left[\, r_0, \max(\tau)\,\right] \tag{2.9}$$

Note that Eq. (2.9) allows to compute the current values for r in terms of the current value of τ, which in turn, depends explicitly on the current strains (see Eqs. (2.1) and (2.3)).

Finally, the damage index d is explicitly defined in terms of the corresponding current value of the damage threshold, so that it is a monotonically increasing function such that $0 \leq d(r) \leq 1$.

In this work, we will use the following functions:

- *Linear hardening/softening:*

$$d(r) = (1 - H_d)\left(1 - \frac{r_0}{r}\right) \qquad r_0 \leq r \tag{2.10}$$

- *Exponential hardening/softening:*

$$d(r) = 1 - \frac{r_0}{r}\exp\left\{2H_d\left(\frac{r}{r_0} - 1\right)\right\} \qquad r_0 \leq r \tag{2.11}$$

where H_d is a constant. When softening is considered ($H_d < 0$), the fracture energy of the material G_f and the characteristic length l_{ch} must be introduced to ensure mesh-size objective results (see below).

It is also possible to express the damage laws in the form (Oliver 2000, Faria et al 2001):

$$d(r) = 1 - \frac{q(r)}{r} \qquad r_0 \leq r \tag{2.12}$$

and they call function $q = q(r) = (1 - d(r))\,r$ the stress-like *hardening/softening function*. In this format, the hardening/softening laws can be rewitten as

- *Linear hardening/softening:*

$$q(r) = H_d(r - r_0) + r_0 \qquad r_0 \leq r \tag{2.13}$$

- *Exponential hardening/softening:*

$$q(r) = r_0 \exp\left\{2H_d\left(\frac{r - r_0}{r_0}\right)\right\} \qquad r_0 \leq r \tag{2.14}$$

Figures 3 and 4 show a schematic representation of these functions for the hardening ($H_d > 0$) and softening ($H_d < 0$) cases.

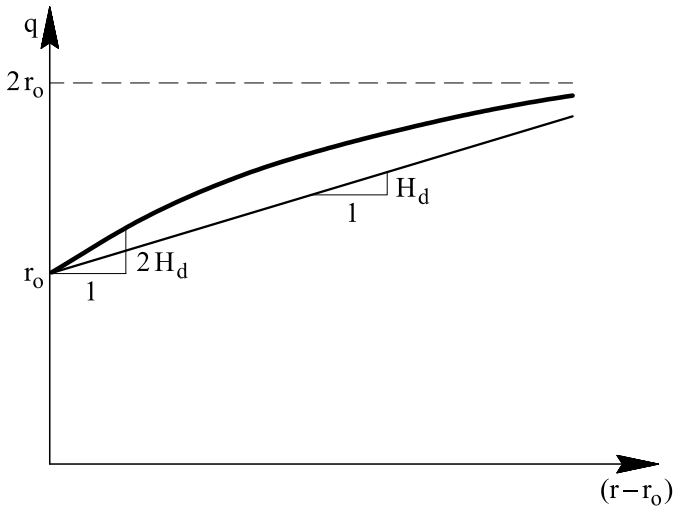

Figure 3 Linear and exponential hardening functions

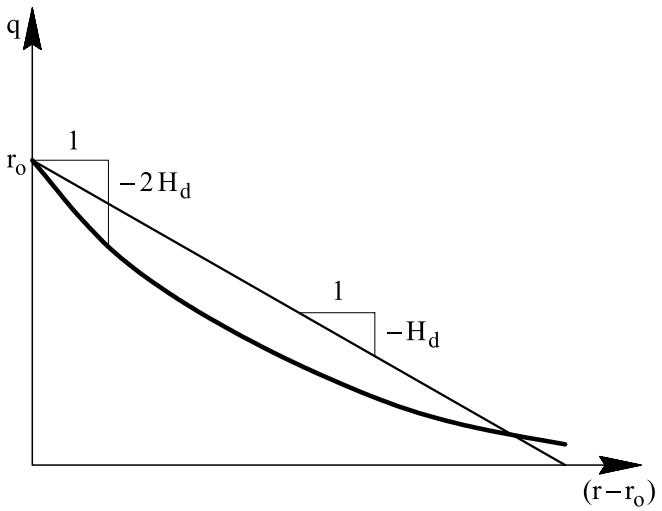

Figure 4 Linear and exponential softening functions

Rate dependent damage

In many materials there is a strong coupling between nonlinear rate-sensitivity and damage growth. Therefore, it is natural to develop a rate dependent constitutive model within the framework of CDMT, evolving from the above presented rate independent damage model, and which accounts for strain rate dependency via the damage evolution laws [Cervera et al. 1996].

To this end, let us consider a viscous regularization of the rate-independent damage threshold evolution law defined by Eq. (2.8), so that this is replaced by:

$$\dot{r} = \frac{\phi(\tau - r)}{\vartheta} \geq 0 \tag{2.15}$$

where $\phi(\cdot)$ is a scalar function called the viscous damage threshold flow function; ϑ is the retardation time for damage. Note that the modification of the evolution law only affects the integration of the damage threshold (r), but not the damage variable (d) itself. This is still obtained in a closed form, through the explicit definition of the function $d(r)$. Additionally, it is worth to remark that Eq. (2.15) must guarantee monotonic increasing of the damage threshold, and, therefore, also of the damage index ($\dot{d} \geq 0$).

It must be noted that the definition of the evolution law (2.15) replaces the Kuhn-Tucker and consistency conditions, Eqs. (2.7a) and (2.7b), of the rate independent model.

The viscous threshold damage flow function may assume the form:

$$\phi(\tau - r) = r_0 \left\langle \frac{\tau - r}{r_0} \right\rangle^a \tag{2.16}$$

where $\langle \cdot \rangle$ are the Macaulay brackets and a is a positive exponent, also a material property. The determination of this exponent, as well as that of the retardation time is done by means of 1D tests. Note that this definition ensures that expression (2.15) is dimensionally correct. This is necessary for ϑ to retain its physical meaning of retardation time for the evolution of damage.

The reasoning behind the above law is analogous to the classical Perzyna viscoplastic regularization often used in the framework of Computational Plasticity. It can be seen that this assumed rate dependent formulation is a general form for the damage threshold and damage evolution, so that for a very small value of the retardation damage parameter, the rate-independent (or inviscid) damage evolution law is recovered, while for an infinite value of ϑ, evolution of the damage

variables is prevented, thus rendering an instantaneously elastic response.

The rate-dependent model can also be written in a Duvaut-Lions format, as

$$\dot{r} = \frac{\phi\,(r_\infty - r)}{\vartheta} \geq 0 \tag{2.17}$$

where r_∞ is the value of the damage threshold corresponding to the current value of τ as $t/\vartheta \to \infty$. As the rate-dependent (viscous) model relaxes to the rate-independent (inviscid) solution, it is obvious that in the inviscid limit, satisfaction of the consistency condition ensures that $r_\infty = \tau$. Therefore, Ecs. (2.15) and (2.17) are completely equivalent.

Thermodynamic Framework

Let us define the elastic free energies associated with the effective stresses in the form

$$W_e \;=\; W_e(\boldsymbol{\varepsilon}) \;=\; \frac{1}{2}\,\overline{\boldsymbol{\sigma}} : \mathbf{D}^{-1} : \overline{\boldsymbol{\sigma}} \quad \geq 0 \tag{2.18}$$

The mechanical free energy term for the damage model is defined in the form:

$$W = W(\boldsymbol{\varepsilon}, d) = (1-d) W_e(\boldsymbol{\varepsilon}) \tag{2.19}$$

where d is the damage index. From this, and recalling that $0 \leq d \leq 1$, it is obvious that $W \geq 0$.

The constitutive equation for the damage model is obtained using Coleman's method as:

$$\boldsymbol{\sigma} = \quad \partial_\varepsilon W \;=\; (1-d)\,\overline{\boldsymbol{\sigma}} \tag{2.20}$$

The mechanical dissipation can be expressed as

$$\dot{D}_{\text{mech}} \;=\; W_e\,\dot{d} \quad \geq 0 \tag{2.21}$$

provided that the damage index increases monotonically, $\dot{d} \geq 0$.

Softening behaviour

Expressions (2.10) and (2.11) are able to reproduce the softening branch that occurs in a 1D tensile or compression test

after the peak stress is reached, with the stress decreasing asymptotically to the strain axis. With these evolution laws for d, a finite area is retained between the stress-strain curve and the strain axis. This area defines the available energy to be dissipated in the control volume. As it is well known, this energy has to be appropriately related to the fracture energy of the material (regarded to be a material property) to satisfy the requisites of mesh-objectivity when dealing with softening materials. The fundamental issue here is the introduction of a geometrical factor, $l_{\rm ch}$, called *characteristic length*, which depends on the spatial discretization and ensures conservation of the energy dissipated by the material [Oliver 1989]. Therefore, the determination of the softening parameter H_d is made by equating the material fracture energy *per unit of characteristic length* to the time integral of dissipation, as follows:

Rate independent behaviour

Consider an experiment in which the load increases *monotonically* and *quasi-statically* from an initial unstressed state to another in which full degradation takes place. Using the rate independent version of the model, the specific energy dissipated in the process is:

$$D_{\rm mech} = \int_{t=0}^{t=\infty} \dot{D}_{\rm mech}\, dt \tag{2.22}$$

$$= \int_{t=0}^{t=\infty} W_e\ \dot{d}\, dt \tag{2.23}$$

$$= \int_{r=r_0}^{r=\infty} \frac{f_e^2}{2E}\, r^2 d'\, dr \tag{2.24}$$

where we have used Eqs. (2.21), (2.18), (2.1), (2.3), (2.9) and the rate of damage can be expressed as $\dot{d} = d'\,\dot{r}$.

We will consider in the following both the cases of linear and exponential softening.

- *Linear softening*

  Using Eq. (2.10), we have $d' = (1 - H_d)\, r_0/r^2$, for $r_0 \leq r \leq r_u$, with $r_u = r_0\,(1 - 1/H_d)$, and $d' = 0$, otherwise. Recalling that $r_0 = 1$, integrating and equating $D_{\rm mech} = G_f\,/l_{\rm ch}$, we have

  $$D_{\rm mech} = \left(1 - \frac{1}{H_d}\right) \frac{f_e^2}{2E} = \frac{G_f}{l_{\rm ch}} \tag{2.25}$$

  and, therefore,

  $$H_d = -\frac{\overline{H}\, l_{\rm ch}}{1 - \overline{H}\, l_{\rm ch}} \qquad \leq 0 \tag{2.26}$$

where $\overline{H} = (f_e)^2 / 2EG_f$ depends on the material properties, as G_f is the fracture energy per unit area, f_e is the uniaxial strength and E is the elastic modulus.

- *Exponential softening*

  Using now Eq. (2.11), we have the damage derivative $d' = (r_0 + 2H_d r) \exp\left\{2H_d \left(\frac{r}{r_0} - 1\right)\right\} / r^2$, for $r_0 \leq r \leq \infty$. Recalling that $r_0 = 1$, integrating and equating $D_{\text{mech}} = G_f / l_{\text{ch}}$, we have

$$D_{\text{mech}} = \left(1 - \frac{1}{H_d}\right) \frac{f_e^2}{2E} \tag{2.27}$$

  which is identical to the result in (2.25).

In the framework of *local* models and finite element analysis, the state variables are computed at the integration points in terms of the local strain (and/or stress) history. Therefore, the threshold and damage internal variables are defined at the integration points. The characteristic length is thus related to the volume (or area) of each finite element. In this work its value will be approximated by the cubic (or square) root of this volume (or area). It is clear from Eq. (2.26) that the introduction of the characteristic length implies a limitation on the maximum size of the finite elements used in the mesh, $l_{\text{ch}} \leq 1/\overline{H}$. The greater the elements, the steeper is the softening branch of the response, and, locally, the fracture process is more brittle.

Note that defining a new hardening parameter in the form $\mathcal{H}_d = -\overline{H}\, l_{\text{ch}}$, or, equivalently, $\mathcal{H}_d = H_d/(1 - H_d)$,the mechanical dissipation can be expressed simply as

$$D_{\text{mech}} = -\frac{1}{\mathcal{H}_d} \frac{f_e^2}{2E} \geq 0 \tag{2.28}$$

It must be remarked that the use of regularized softening parameters is intended to achieve results which are independent of the element size. However, they can not eliminate another great inconvenience of softening defined al local level, the dependency of the results on the orientation of the mesh, or *mesh bias*, a fact almost impossible to avoid in a practical computations, under the assumptions of standard continuum mechanics [Oliver et al. 1992].

Rate dependent behaviour

Let us now consider an experiment in which the load increases *monotonically,* and *not quasi-statically* from an initial unstressed state to another in which full degradation takes place. Using the rate dependent version of the model, the specific energy dissipated in the process is:

$$D_{\text{mech}} = \int_{t=0}^{t=\infty} \dot{D}_{\text{mech}}\, dt \tag{2.29a}$$

$$= \int_{t=0}^{t=\infty} W_e\ \dot{d}\, dt \tag{2.29b}$$

$$= \int_{r=r_0}^{r=\infty} \frac{f_e^2}{2E} \left[r + r_0 \left(\frac{\vartheta \dot{r}}{r_0} \right)^{\frac{1}{a}} \right]^2 d'\, dr \tag{2.29c}$$

where we have used Eqs. (2.21), (2.18), (2.1), and also Eqs. (2.15) and (2.16) and the rate of damaged can be expressed as $\dot{d} = d' \dot{r}$.

Comparing Eq. (2.29c) with Eq. (2.24) it is obvious that the first one reduces to the second for very small values of ϑ, or for very slow processes, with $\dot{r}$ tending to zero. In other cases, the governing laws, Eqs. (2.15) and (2.16), ensure that the terms r and $r_0 \left(\vartheta \dot{r}/r_0\right)^{\frac{1}{a}}$ are of the same order, that is $\left(\vartheta \dot{r}\right)^{\frac{1}{a}} / r = O(1)$. Therefore, it can be assumed that the regularized parameter from Eq. (2.26), that regularizes the rate independent model, will also regularize the rate dependent model, both for linear and exponential softening.

It must be remarked that formats of the regularized damage law different from that of Eq. (2.16) may lead to the necessity of regularizing *also* the retardation damage parameter ϑ, making it dependent on the element size (Bicanic 1990, Cervera et al 1996).

Integration of the internal variables

A numerical algorithm needs to be implemented for the time integration of the damage constitutive equations presented in the previous Sections. In the following this algorithm is presented, in a strain–driven form which leads to an almost closed–form algorithm to integrate the stress tensor in time. This is most appropriate within the context of the application of the finite element method.

Each time step begins at time t_n with all state variables known and it ends at time t_{n+1} with the state variables updated according to the given total strain tensor $\boldsymbol{\epsilon}$. The time step size is $\Delta t = t_{n+1} - t_n$.

For the rate independent model, Eq. (2.9) allows to compute the current value for r_{n+1} in terms of the current value of τ_{n+1}, which in turn, depends explicitly on the current strains $\boldsymbol{\epsilon}_{n+1}$(see Eqs. (2.1) and (2.3)). After this, the damage index d_{n+1} is explicitly computed in terms of the corresponding current value of the damage threshold, using the appropriate expression, Eqs. (2.10) or (2.11).

For the rate dependent model, the only difference is the updating of the damage thresholds when evolution of the damage occurs, that is, upon loading conditions. These may be evaluated using a generalized mid-point rule to integrate Eq. (2.15), i.e.,

$$r_{n+1} \;=\; r_n + \frac{\Delta t}{\vartheta}\,\phi(\tau_\alpha - r_\alpha) \tag{2.30}$$

where τ_α and r_α are defined by:

$$\tau_\alpha \;=\; (1-\alpha)\,\tau_n + \alpha\,\tau_{n+1} \tag{2.31a}$$
$$r_\alpha \;=\; (1-\alpha)\,r_n + \alpha\,r_{n+1} \tag{2.31b}$$

For the sake of shortness, we can write Eq. (2.30) as:

$$r_{n+1} \;=\; r_n + \Delta r_{n+1} = \; r_n + \frac{\Delta t}{\vartheta}\,\phi_\alpha \tag{2.32}$$

where ϕ_α represents the value of function ϕ evaluated at time α, that is

$$\phi_\alpha \;=\; \phi\,(\tau_\alpha - r_\alpha) \tag{2.33a}$$
$$\;=\; \phi\,[(1-\alpha)(\tau_n - r_n) + \alpha(\tau_{n+1} - r_{n+1})] \tag{2.33b}$$

Note that for $\alpha = 1$ Eq. (2.32) corresponds to a backward-Euler difference scheme. It is easy to show that the algorithm of Eq. (2.32) is unconditionally stable for $\alpha \geq 0.5$ and second order accurate only for $\alpha = 0.5$ (Crank-Nicholson or trapezoidal rule), which allows the use of larger time step sizes for rate-dependent analysis.

It is obvious that the explicit determination of r_{n+1} is possible only for small integer values of the exponent a in Eq. (2.16), as the cases $a = 1, 2, 3$ lead to linear, quadratic and cubic expressions for Eq. (2.32), respectively. For instance, for $a = 1$ it is

$$\Delta r_{n+1} \;= \frac{\frac{\Delta t}{\vartheta}\,[(1-\alpha)(\tau_n - r_n) + \alpha(\tau_{n+1} - r_{n+1})]}{1 + \alpha\frac{\Delta t}{\vartheta}} \tag{2.34}$$

In the general case, Eq. (2.32) may be solved by the iterative Newton-Raphson method, which ensures a fast rate of convergence. To this purpose, Eq. (2.32) may be rewritten as:

$$f(r_{n+1}) \;=\; 0 \;=\; -r_{n+1} \,+\, r_n + \frac{\Delta t}{\vartheta}\,\phi_\alpha \tag{2.35}$$

so that the problem is now to find the root of Eq. (2.35) by an iterative Newton-Raphson procedure given by:

$$r_{n+1}^{i+1} \;=\; r_{n+1}^{i} - \frac{f(r_{n+1}^{i})}{f'(r_{n+1}^{i})} \tag{2.36}$$

where r_{n+1}^{i+1} indicates an improved approximation to the exact root obtained from the previous r_{n+1}^{i+1} approximation and f' is the first derivative of function f with respect to r_{n+1}. This leads to the iterative update of the increment Δr_{n+1} in the form

$$\Delta r_{n+1}^{i+1} \;= \frac{\frac{\Delta t}{\vartheta}\left[\phi_\alpha + \alpha\,\phi'_\alpha\,\Delta r_{n+1}^{i}\right]}{1+\alpha\frac{\Delta t}{\vartheta}} \tag{2.37}$$

where ϕ'_α represents the value of the derivative of function ϕ evaluated at time α. The iteration procedure starts for $i = 0$ with $\Delta r_{n+1}^{0} = 0$ and finishes when a preselected convergence criterion is satisfied.

A useful alternative to the use of the Newton-Raphson procedure is the linealization of Ec. (2.33a) in the form

$$\begin{aligned} \phi_\alpha \;&\simeq\; \phi_n + \phi'_n \cdot [(\tau_\alpha - r_\alpha) - (\tau_n - r_n)] && \text{(2.38a)}\\ &=\; \phi_n + \alpha\,\phi'_n \cdot [(\tau_{n+1} - \tau_n) - (r_{n+1} - r_n)] && \text{(2.38b)} \end{aligned}$$

This leads to an explicit update of the increment Δr_{n+1} in the form

$$\Delta r_{n+1} \;= \frac{\frac{\Delta t}{\vartheta}\left[\phi_n + \alpha\,\phi'_n \cdot (\tau_{n+1} - \tau_n)\right]}{1+\alpha\frac{\Delta t}{\vartheta}} \tag{2.39}$$

Note that in Eq. (2.30) the condition to update the damage threshold is $\tau_\alpha > r_\alpha$. However, r_α cannot be computed before a new value for r_{n+1} is found. Therefore, the previous condition is changed in the algorithm by an alternative check, $\tau_\alpha > r_n$. Consequently, once a converged value for r_{n+1} has been computed according to the described procedure, Eq. (2.31b) is used to evaluate the corresponding r_α value. Then a check is performed to ensure that the condition $\tau_\alpha > r_\alpha$ is satisfied. Otherwise, there is no evolution of damage in the time step and, therefore, $r_{n+1} = r_n$.

Differentiating Eq.(2.2) with respect to time, we obtain

$$\dot{\boldsymbol{\sigma}} = \ (1-d)\,\dot{\overline{\boldsymbol{\sigma}}} - \dot{d}\overline{\boldsymbol{\sigma}} \tag{2.40}$$

Also, differentiating Eq.(2.1) with respect to time, we have

$$\dot{\overline{\boldsymbol{\sigma}}} = \mathbf{D} : \dot{\boldsymbol{\varepsilon}} \tag{2.41}$$

On the other hand, the time derivative of the damage index is

$$\dot{d} = d'\,\dot{r} \tag{2.42}$$

where the derivative d' can be obtained from Eqs.(2.10)-(2.11). On loading, consistency requires that $\dot{r} = \dot{\tau}$, and therefore, differentiating Eq. (2.3), we can write

$$\dot{r} = \dot{\tau} = \frac{1}{f_e^2}\frac{1}{\tau}\left[\,\overline{\boldsymbol{\sigma}} :\, \mathbf{C} : \dot{\overline{\boldsymbol{\sigma}}}\right] \tag{2.43}$$

On unloading, it is $\dot{r} = 0$. Substituting this result in Eq. (2.42), and the result in Eq. (2.40), yields the desired expression

$$\dot{\boldsymbol{\sigma}} = \mathbf{D}^{\tan} : \dot{\boldsymbol{\varepsilon}} \tag{2.44}$$

with

$$\mathbf{D}^{\tan} = [\,(1-d)\,\mathbf{I} - h\,(\overline{\boldsymbol{\sigma}} \otimes \overline{\boldsymbol{\sigma}}) :\, \mathbf{C}] : \mathbf{D} \tag{2.45}$$

where the coefficient h is

$$h = \begin{cases} \dfrac{1}{f_e^2}\dfrac{d'}{\tau} & \text{for loading} \\ \\ 0 & \text{for unloading} \end{cases} \tag{2.46}$$

Note that, for an arbitrary selection of tensor $\mathbf{C}$, this tangent operator is non-symmetric, as it corresponds to a *non-associative damage law*. However, for the particular choice of $\mathbf{C} = \overline{\mathbf{D}}^{-1} = (\mathbf{D}/E)^{-1}$ [Simó and Ju 1987a], the corresponding *damage law* is associative, and the tangent operator is symmetric:

$$\mathbf{D}^{\tan} = \ (1-d)\,\mathbf{D} - h\,E\,(\overline{\boldsymbol{\sigma}} \otimes \overline{\boldsymbol{\sigma}}) \tag{2.47}$$

Rate dependent damage

In the case of rate dependent damage the determination of $\dot{r}$ comes from differentiating Eq. (2.32) with respect to time, to yield:

$$\dot{r} = \frac{\alpha \frac{\Delta t}{\vartheta} \phi'_\alpha}{1 + \alpha \frac{\Delta t}{\vartheta} \phi'_\alpha} \dot{\tau} \tag{2.48}$$

where ϕ'_α represents the value of the derivative of function ϕ evaluated at time α. Note that when using the approximation of Ec. (2.38a), $\phi'_\alpha \simeq \phi'_n$. Comparing Eqs. (2.43) and (2.48), it is obvious that the tangent operator for the rate dependent damage case has the same expression of Eq. (2.45) with the coefficient h given by

$$h = \begin{cases} \dfrac{\alpha \frac{\Delta t}{\vartheta} \phi'_\alpha}{1 + \alpha \frac{\Delta t}{\vartheta} \phi'_\alpha} \dfrac{1}{f_e^2} \dfrac{d'}{\tau} & \text{for loading} \\ 0 & \text{for unloading} \end{cases} \tag{2.49}$$

Note that for large values of $\Delta t/\vartheta$ the rate independent case is recovered.

Coupling with visco-elasticity

Let us now consider the coupling of the viscoelastic model described in Chapter 1 with the damage model described above. The basic hypothesis is that the stress sustained by the Maxwell chain is the effective (undamaged) stress, rather than the total stress (see Figure 5). This idea is based on the CDMT concept that it is the effective stress the one acting on the effective (undamaged) solid concrete, while the total stress acts on the whole (damaged) solid [Cervera et al. 1992].

Let us begin by defining the effective stresses and the elastic strains for one element of the Maxwell chain as:

$$\overline{\boldsymbol{\sigma}}^i = \xi^i \mathbf{D} : (\boldsymbol{\varepsilon} - \boldsymbol{\varepsilon}^i) \tag{2.50}$$

with $\xi^i = E^i/E$ being the participation factor of $i-th$ element, and $\boldsymbol{\varepsilon}^i$ being the viscous strains in each Maxwell element, with the evolution law:

$$\dot{\boldsymbol{\varepsilon}}^i = \frac{1}{\vartheta^i} (\boldsymbol{\varepsilon} - \boldsymbol{\varepsilon}^i) \qquad \text{for} \quad i = 0, 1, ..., N \tag{2.51}$$

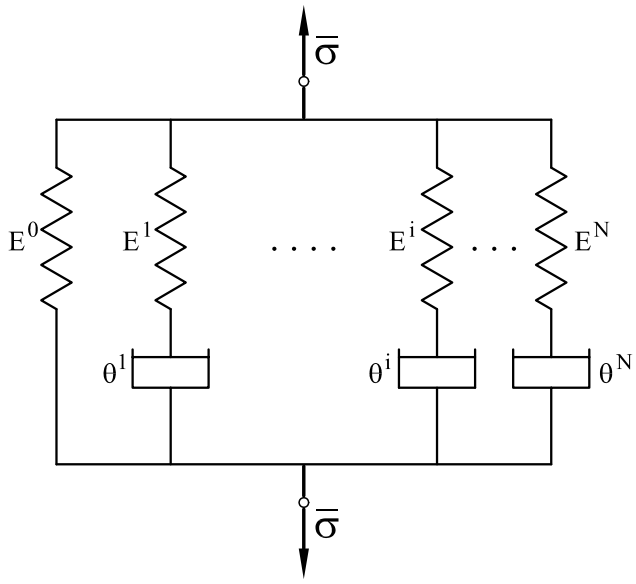

Figure 5 Maxwell chain subjected to effective stress

where ϑ^i are the relaxation times of the corresponding dashpots.

Let us define the elastic free energy for each element in the form

$$W_e^i = W_e^i(\boldsymbol{\varepsilon}, \boldsymbol{\varepsilon}^i) \;=\; \frac{1}{2}\,\overline{\boldsymbol{\sigma}}^i : (\xi^i\,\mathbf{D})^{-1} : \overline{\boldsymbol{\sigma}}^i \tag{2.52}$$

The total elastic free energy associated to the Maxwell chain is obtained by adding the contributions of the elements

$$W_e \;=\; W_e(\boldsymbol{\varepsilon},\boldsymbol{\varepsilon}^i) = \sum_{i=0}^{N} W_e^i(\boldsymbol{\varepsilon}, \boldsymbol{\varepsilon}^i) \tag{2.53}$$

Introducing the damage index d, the mechanical free energy is defined in the form:

$$W = W(\boldsymbol{\varepsilon}, \boldsymbol{\varepsilon}^i, d) = (1-d)\, W_e(\boldsymbol{\varepsilon}, \boldsymbol{\varepsilon}^i) \;\geq 0. \tag{2.54}$$

The stresses are obtained as:

$$\boldsymbol{\sigma} = \partial_\varepsilon W \;=\; (1-d) \sum_{i=0}^{N} \overline{\boldsymbol{\sigma}}^i \tag{2.55a}$$

$$\;=\; (1-d)\,\overline{\boldsymbol{\sigma}} \tag{2.55b}$$

so that the same final form as in Eq. (2.2) is obtained for the damage model.

The definition of the damage surfaces and the evolution of the damage indices and thresholds can be done as explained previously.

The mechanical dissipation can be split into its viscoelastic and damage parts, in the form:

$$\mathcal{D}_{\text{mech}} = \sum_{i=0}^{N} \frac{2}{\vartheta^i} W_e^i + W_e \dot{d} \geq 0 \tag{2.56}$$

Tangent operator

The constitutive equation can also be written as

$$\begin{aligned}
\boldsymbol{\sigma} &= (1-d)\,\overline{\boldsymbol{\sigma}} && (2.57a)\\
&= (1-d)\left[\sum_{i=0}^{N} \overline{\boldsymbol{\sigma}}^i\right] && (2.57b)\\
&= (1-d)\left[\sum_{i=0}^{N} \xi^i \mathbf{D} : (\boldsymbol{\varepsilon} - \boldsymbol{\varepsilon}^i)\right] && (2.57c)\\
&= (1-d)\left[\mathbf{D} : \boldsymbol{\varepsilon} - \sum_{i=0}^{N} \xi^i \mathbf{D} : \boldsymbol{\varepsilon}^i\right] && (2.57d)\\
&= (1-d)\left[\mathbf{D} : \boldsymbol{\varepsilon} - \overline{\boldsymbol{\sigma}}^{\text{visc}}\right] && (2.57e)
\end{aligned}$$

where $\overline{\boldsymbol{\sigma}}^{\text{visc}} = \sum_{i=0}^{N} \xi^i \mathbf{D} : \boldsymbol{\varepsilon}^i$. Differentiating Eq. (2.57e) with respect to time, we have

$$\dot{\boldsymbol{\sigma}} = (1-d)\left[\mathbf{D} : \dot{\boldsymbol{\varepsilon}} - \dot{\overline{\boldsymbol{\sigma}}}^{\text{visc}}\right] - \dot{d}\left[\mathbf{D} : \boldsymbol{\varepsilon} - \overline{\boldsymbol{\sigma}}^{\text{visc}}\right] \tag{2.58}$$

Differentiating the integration scheme for the viscous strains, Eq. (1.15) we obtain

$$\begin{aligned}
\dot{\overline{\boldsymbol{\sigma}}}^{\text{visc}} &= \sum_{i=0}^{N} \xi^i \mathbf{D} : \dot{\boldsymbol{\varepsilon}}^i && (2.59)\\
&= \left[\sum_{i=0}^{N} \xi^i e^{-\frac{\Delta t}{\vartheta^i}}\right] \mathbf{D} : \dot{\boldsymbol{\varepsilon}} && (2.60)
\end{aligned}$$

Using these results, together with previously obtained results for $\dot{d}$, we can write:

$$\dot{\boldsymbol{\sigma}} = \mathbf{D}^{\text{tan}} : \dot{\boldsymbol{\varepsilon}} \tag{2.61}$$

with the tangent operator consistent with the numerical integration schemes proposed being:

$$\mathbf{D}^{\text{tan}} = (1-d)\,\mathbf{D}^{\text{visc}} - h\,E\left(\overline{\boldsymbol{\sigma}} \otimes \overline{\boldsymbol{\sigma}} + \overline{\boldsymbol{\sigma}} \otimes \overline{\boldsymbol{\sigma}}^{\text{visc}}\right) \tag{2.62}$$

where $\mathbf{D}^{\text{visc}}$ is that of Eq. (1.18):

$$\mathbf{D}^{\text{visc}} = \left[\sum_{i=0}^{N} \xi^i e^{-\frac{\Delta t}{\vartheta^i}}\right] \mathbf{D} \tag{2.63}$$

and the coefficients h are those given in Eqs. (2.46) or (2.49), depending on the rate dependency of the damage.

Note the additional unsymmetrical term, $\overline{\boldsymbol{\sigma}} \otimes \overline{\boldsymbol{\sigma}}^{\text{visc}}$, that appears in Eq. (2.62), as compared with Eq. (2.47). If this unsymmetrical coupling term between viscoelasticity and damage is neglected, we have an *approximate* tangent operator, and it will not render quadratic convergence when used in a Newton-Raphson iterative scheme.

Numerical examples

In order to verify the performance of the constitutive isotropic damage model described above, some numerical examples are presented.

These examples focus on the influence of the parameters defining the model on the obtained behaviour. The parameters needed to define the model are summarized in Table 2.1. In this Table, reference to the different material properties is made both in the notation used in the text and with the names of the variables that the finite element program COMET [Cervera et al. 2002] uses to denote the corresponding parameters.

Name	**Text**	**Variable**
Young's modulus	E	`YOUNG`
Poisson's ratio	ν	`POISS`
Tensile/compressive strength	f_e	`STREN`
Hardening/Softening law[1]	–	`ILAWT`
Linear hardening parameter	–	`HFACT`
Tensile fracture energy	G_f	`GFRAC`
Retardation timefor damage	ϑ	`RETAT`
Number of Maxwell chains	N	`NMAXW`
Elasticity modulus ratio for chain i	ξ^i	`ELASi`
Relaxation time for chain i	ϑ^i	`RETAi`

Table 2.1 Parameters used in the model

To conduct the desired tests on the numerical integration of the constitutive model a finite element model must be defined, together with the appropriate boundary and loading conditions.

To this end, a FE mesh consisting of a single four-noded element of 1×1 m in the $x - y$ plane, simply (isostatically) supported is used. Plane strain conditions are assumed in the z-direction. The element is loaded in x-direction by imposing a prescribed displacement that follows the cyclic time history shown in Figure 6. A constant time step size of $\Delta t = 10$ s was used to perform the analyses.

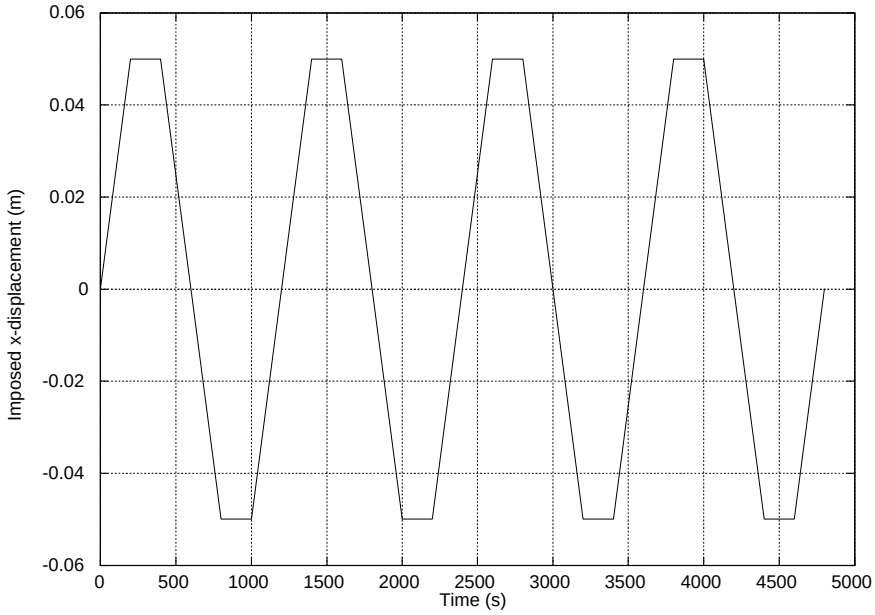

Figure 6 Cyclic load

Rate dependency

Two different cases are defined to study the influence of the retardation time for damage. The values used in the models are showed in Table 2.2. Two different values of the linear hardening parameter are used in each case. All units are in the SI system. Note that in Case 1 damage growth is rate

Variable	**Case 1**	**Case 2**
YOUNG	100 000	100 000
POISS	0.3	0.3
STREN	2 500	2 500
ILAWT	0	0
HFACT	0.2 / 0.02	0.2 / 0.02
GFRAC	–	–
RETAT	0	500

Table 2.2 Values of material properties

independent, with $\vartheta = 0$, while in Case 2 damage growth is rate dependent, with $\vartheta = 500$.

Results for Case 1 are shown in Figures 7 and 8. Figure 7 shows the stress evolution in time, compared with a purely elastic behaviour. Figure 8 shows the corresponding stress *versus* strain curve. In this case it can be observed that:

- the onset of damage is evident in the ascending branch of the first cycle, when the corresponding (initial) threshold values is reached. Note that: this is *not* equal to the uniaxial strength, but slightly higher, due to the fact that plane strain conditions and Poisson´s effect induce a state of biaxial effective stresses;
- damage occurs instantaneously, in a rate independent manner;
- for `HFACT` $= 0.2$, the hardening after the onset of damage is clear, while for `HFACT` $= 0.02$, the increase of stress after the initiation of damage is very minor;
- unloading takes place to the origin, with the corresponding damaged stiffness, but without inelastic strains;
- reloading upon load reversal takes place with the same damaged stiffness; and
- subsequent cycles after the first one do not produce any damage growth, as the strain amplitude of the cycles is constant.

Figures 9, and 10 show corresponding results for Case 2. Note that now:

- the onset of damage occurs in the ascending branch of the first cycle, when the corresponding (initial) threshold values is reached;
- damage does not occur instantaneously, as it is delayed by a quite large retardation time;
- stress evolution for both values of `HFACT`is quite similar at the beginning, but it tends to the same difference as for the rate independent case;
- unloading takes place to the origin, with the corresponding damaged stiffness, but without inelastic strains;

- reloading upon load reversal takes place with the same damaged stiffness; and
- subsequent cycles after the first one continue to produce damage growth, delayed by a quite large retardation time, even if the strain amplitude of the cycles is constant.
- the steady state cycle, when reached, is equal to the one in the rate independent case.

Softening behaviour

Two more cases are defined to study the options for softening behavior. The values used in the models are showed in Table 2.3. All units are in the SI system. Two different softening laws are used in each case, `ILAWT`$= 0$ for linear softening and `ILAWT`$= 1$ for exponential softening . Note that in Case 3 damage growth is rate independent, with $\vartheta = 0$, while in Case 4 damage growth is rate dependent, with $\vartheta = 500$.

Variable	**Case 3**	**Case 4**
`YOUNG`	100 000	100 000
`POISS`	0.3	0.3
`STREN`	2 500	2 500
`ILAWT`	0 / 1	0 / 1
`HFACT`	–	–
`GFRAC`	156.25	156.25
`RETAT`	0	500

Table 2.3 Values of material properties

Results for Case 3 are shown in Figures 11 and 12. Figure 11 shows the stress evolution in time, compared with a purely elastic behaviour. Figure 12 shows the stress *versus* strain curve for the exponential case. In this case it can be observed that:

- the onset of damage is evident in the ascending branch of the first cycle, when the corresponding (initial) threshold values is reached. Note that: this is *not* equal to the uniaxial strength, but slightly higher, due to the fact that plane strain conditions and Poisson's effect induce a state of biaxial effective stresses;
- damage occurs instantaneously, in a rate independent manner;
- for `ILAWT`$= 0$ for softening is linear and for `ILAWT`$= 1$ for softening is exponential;

- unloading takes place to the origin, with the corresponding damaged stiffness, but without inelastic strains;
- reloading upon load reversal takes place with the same damaged stiffness; and
- subsequent cycles after the first one do not produce any damage growth, as the strain amplitude of the cycles is constant.

Coupling with viscoelasticity

Finally, two more cases are defined to couple the damage model to the visco-elasticity model described in Chapter 1. The values used in the models are showed in Table 2.4. All units are in the SI system. In Case 5, linear hardening is considered, while in Case 6 linear and exponential softening is compared. In both cases damage growth is computed as rate independent, with $\vartheta = 0$, and as rate dependent, with $\vartheta = 500$.

Variable	**Case 5**	**Case 6**
YOUNG	100 000	100 000
POISS	0.3	0.3
STREN	2 500	2 500
ILAWT	0	0 / 1
HFACT	0.2	–
GFRAC	–	156.25
RETAT	0 / 500	0/500
NMAXW	1	1
ELAS1	0.5	0.5
RETA1	100	100

Table 2.4 Values of material properties

Results for Case 5 are shown in Figures 15 and 16. Figure 15 shows the stress evolution in time, compared with a purely elastic behaviour. Figure 16 shows the stress *versus* strain curve for the rate-dependent damage case. It can be observed that the response is quite realistic, particularly for the rate dependent case. Note how this tends to a steady state cycle which coincide with the rate independent one.

Results for Case 6 are shown in Figures 17, 18, 19 and 20. Figures 17 and 19 show the stress evolution in time for the four different sub-cases, compared with a purely elastic behaviour. Figures 18 and 20 show the stress *versus* strain curve for both sub-cases with exponential softening. Again, the response is

quite realistic, particularly for the rate dependent case. Note how this tends to a steady state cycle which coincide with the rate independent one.

Figures 13 and 14 show corresponding results for Case 4. Note that now:

- the onset of damage occurs in the ascending branch of the first cycle, when the corresponding (initial) threshold values is reached;
- damage does not occur instantaneously, as it is delayed by a quite large retardation time;
- stress evolution for both values of `ILAWT`is quite similar at the beginning, but it tends to the same difference as for the rate independent case;
- unloading takes place to the origin, with the corresponding damaged stiffness, but without inelastic strains;
- reloading upon load reversal takes place with the same damaged stiffness; and
- subsequent cycles after the first one continue to produce damage growth, delayed by a quite large retardation time, even if the strain amplitude of the cycles is constant.
- the steady state cycle, when reached, is equal to the one in the rate independent case.

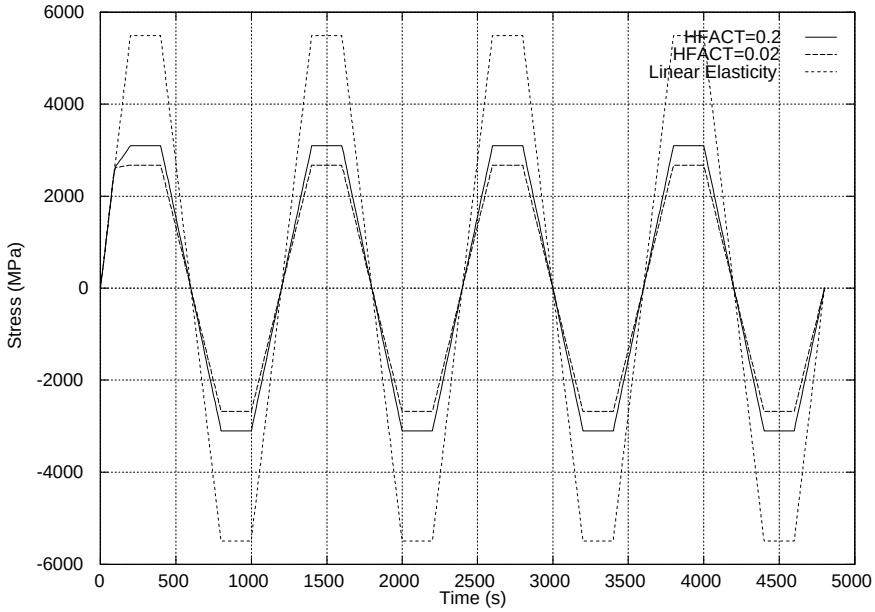

Figure 7 Stress vs. Time for Case 1

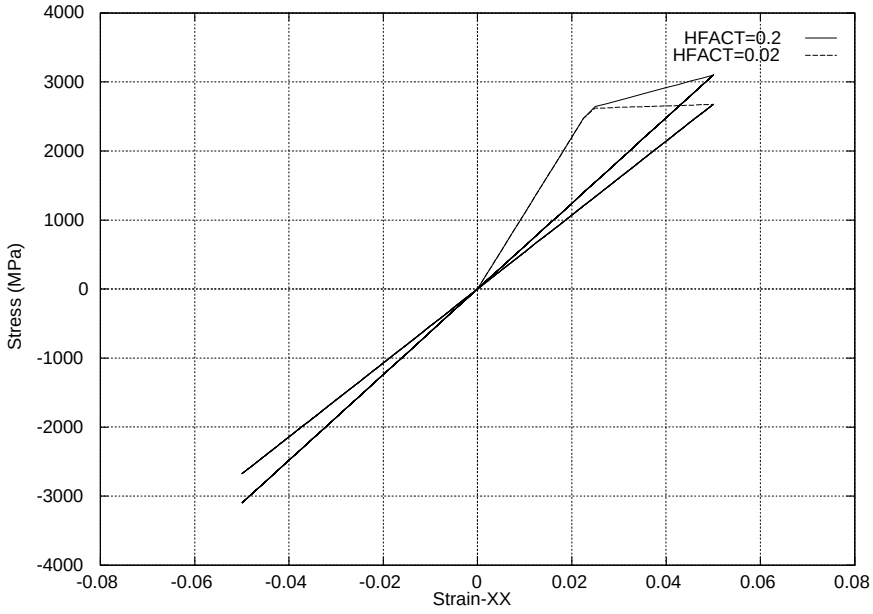

Figure 8 Stress vs. Strain for Case 1

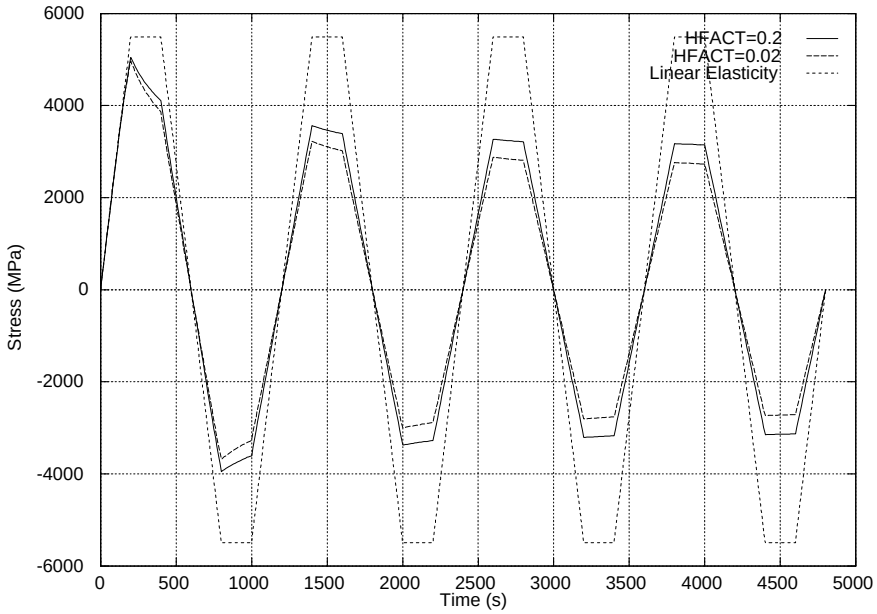

Figure 9 Stress vs. Time for Case 2

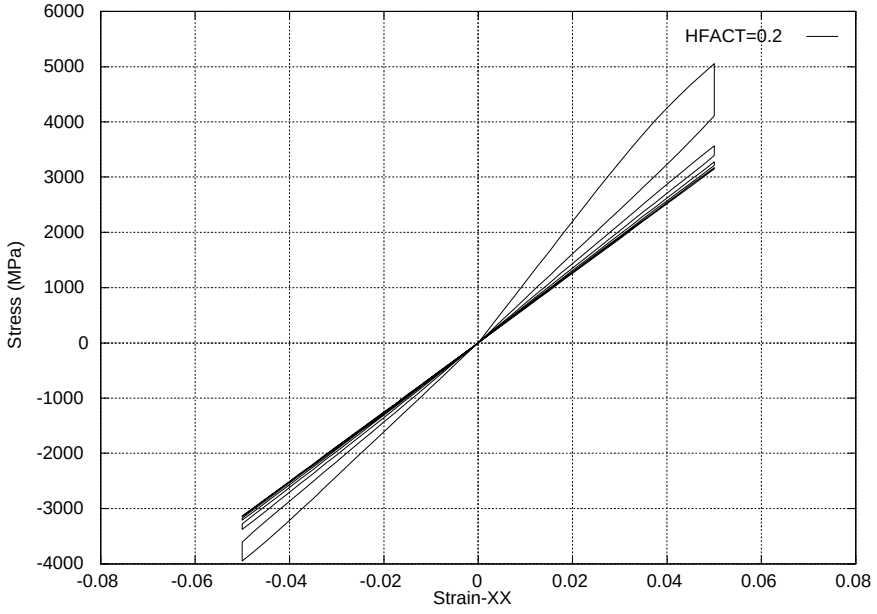

Figure 10 Stress vs. Strain for case 2 (HFACT=0.2)

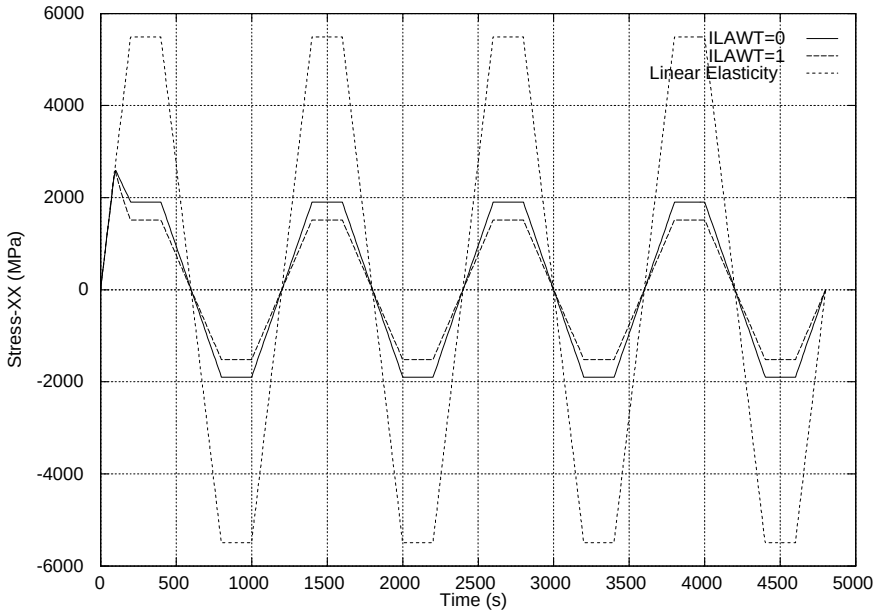

Figure 11 Stress vs. Time for Case 3

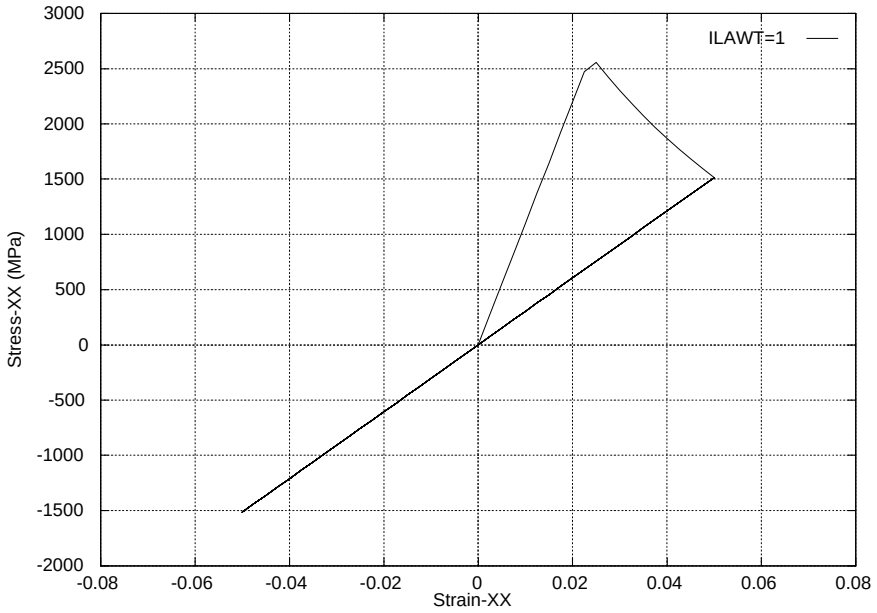

Figure 12 Stress vs. Strain for Case 3 (ILAWT=1)

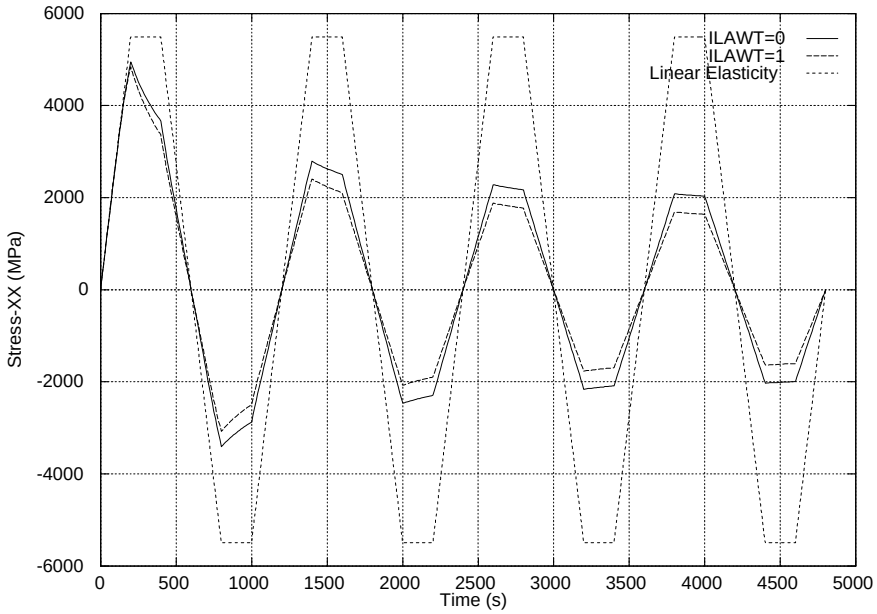

Figure 13 Stress vs. Time for Case 4

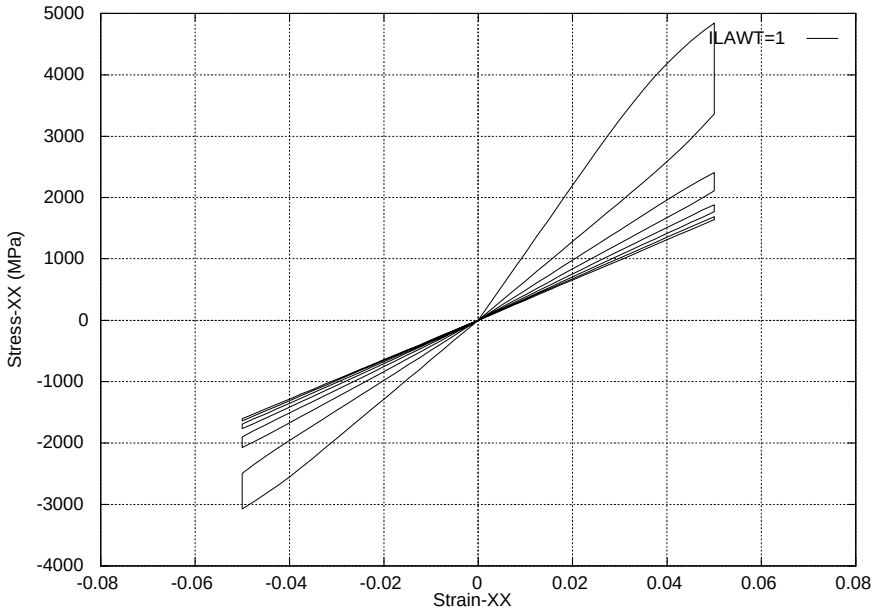

Figure 14 Stress vs. Strain for Case 4 (ILAWT=1)

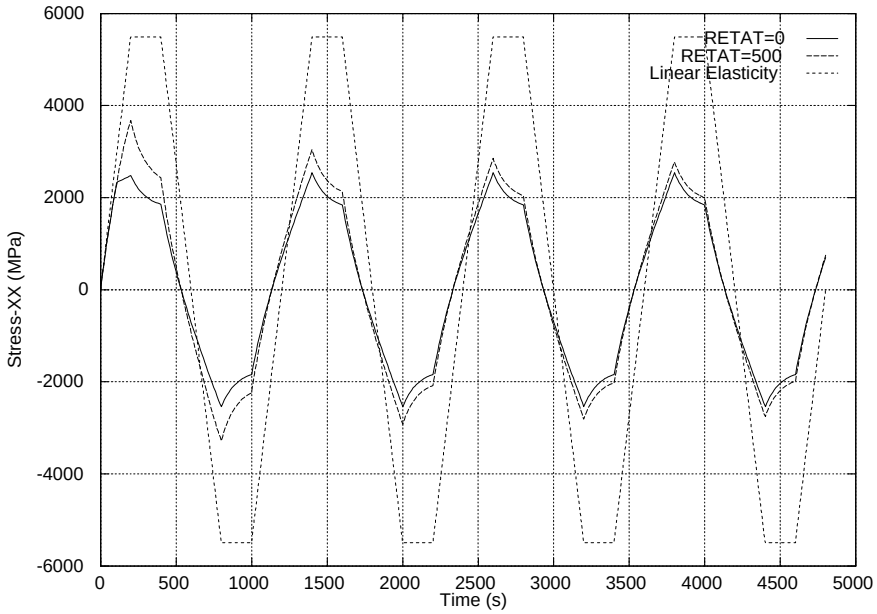

Figure 15 Stress vs. Time for Case 5

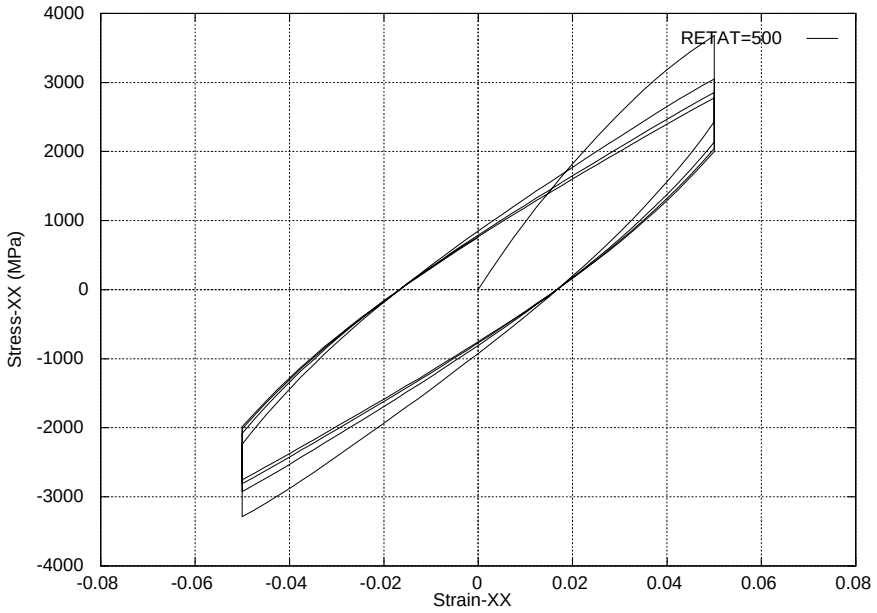

Figure 16 Stress vs. Strain for Case 5 (RETAT=500)

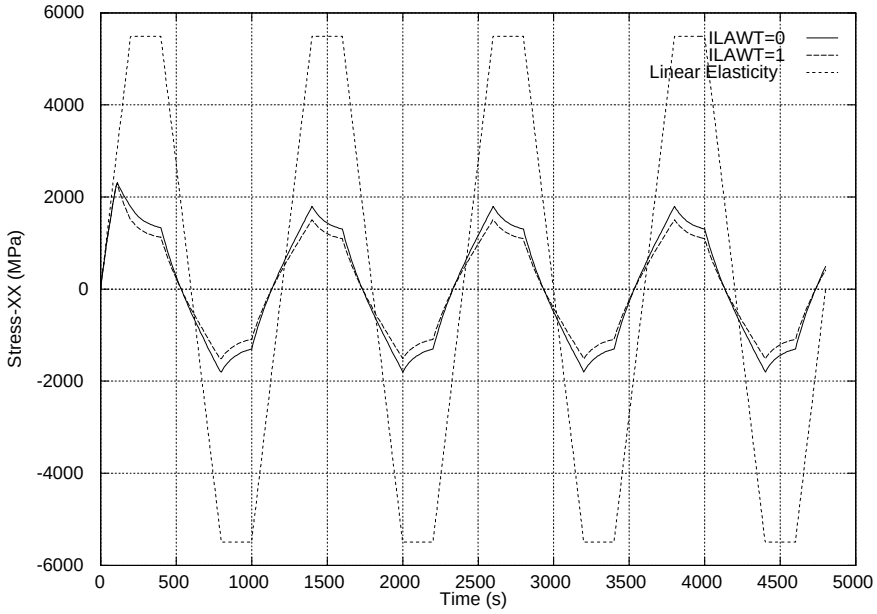

Figure 17 Stress vs. Time for Case 6 (RETAT=0)

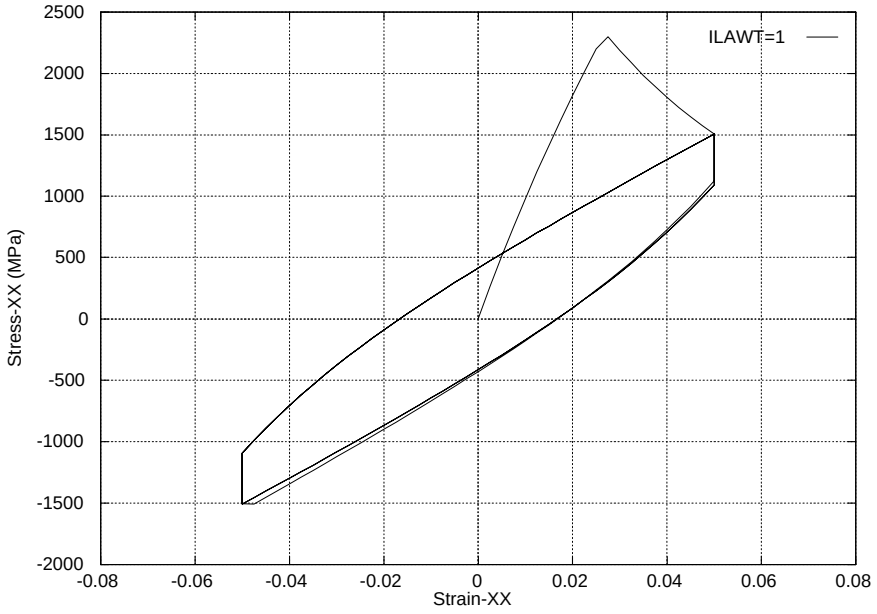

Figure 18 Stress vs. Strain for Case 6 (ILAWT=1,RETAT=0)

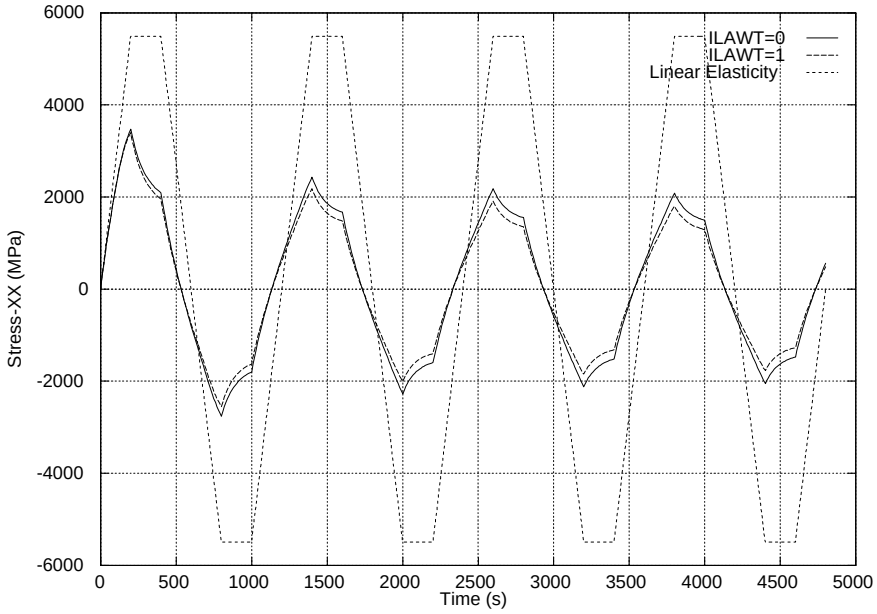

Figure 19 Stress vs. Time for Case 6 (RETAT=500)

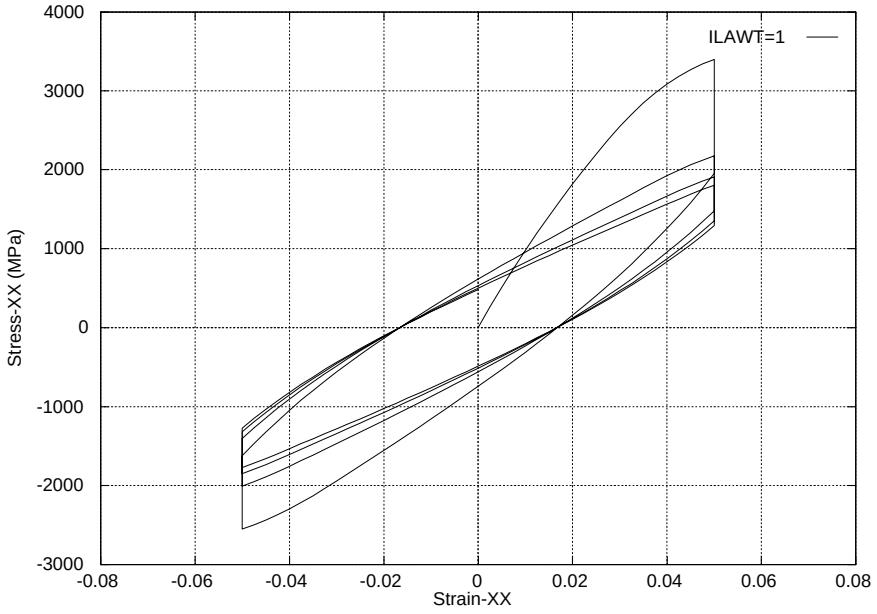

Figure 20 Stress-Strain for Case 6 (ILAWT=1,RETAT=500)

3 TENSION-COMPRESSION DAMAGE

Constitutive model

Introduction

The mechanical behaviour of many geomaterials, like concrete for instance, is complex and highly nonlinear, even for moderate stress levels. A reasonable model should contemplate features such as: (a) large difference in the tensile and compressive strengths, leading to rather distinct stress-strain curves obtained under tension or compression, (b) stiffness recovery upon load sign reversal, that is, passing from tension to compression, or viceversa, (c) strength enhancement under 2D or 3D stress states, when compared to uniaxial tests, (d) rate sensitivity, etc. The available literature includes models based on the theories of hypoelasticity, hyperelasticity, plasticity, fracture mechanics, plastic–fracture, or continuum damage, to name only some of the more popular ones.

Among the different possibilities that such a framework offers (Lemaitre and Chaboche 1978; Lemaitre 1984; Chaboche 1988a,b; Simó and Ju 1987a,b; Mazars and Pijaudier-Cabot 1989, Faria et al. 2001), the present work will make use of a *continuum damage model* to characterize this type of mechanical behaviour. In particular, we will formulate an *isotropic damage model*, with only two scalar internal variables to monitor the local damage under tension and compression, respectively. This will provide a simple constitutive model which, nevertheless, is able to capture the overall non–linear behaviour including strain–hardening/softening response, stiffness degradation and regradation under multiple stress reversals and rate dependency. Furthermore, the model can be implemented in a strain–driven form which leads to an almost closed–form algorithm to integrate the stress tensor in time. This is a most

valuable feature for a model intended to be used in large scale computations. The damage model presented here is an extension of the one described in Cervera et al. (1995, 1996, 1998) and Faria et al. (1998, 2001).

Effective Stresses

The Continuum Damage Mechanics Theory (CDMT) is based on the definition of the effective stress concept, which is introduced in connection with the hypothesis of strain equivalence [Lemaitre and Chaboche 1978]: the strain associated with a damaged state under the applied stress σ is equivalent to the strain associated with its undamaged state under the effective stress $\bar{\sigma}$. In the present work the (second order) effective stress tensor $\overline{\boldsymbol{\sigma}}$ will assume the following hyper-elastic form:

$$\overline{\boldsymbol{\sigma}} = \mathbf{D} : \boldsymbol{\varepsilon} \tag{3.1}$$

where $\boldsymbol{\varepsilon}$ is the (second order) strain tensor, $\mathbf{D}$ is the usual (fourth order) linear–elastic constitutive tensor and (:) denotes the tensor product contracted on two indices.

As our aim is to use a scalar damage model with separated internal damage variables for tensile and compressive stress contributions, a split of the *effective* stress tensor into tensile and compressive components is needed. In order to identify clearly contributions with respect to each one of these independent effective stress tensors, $(+)$ and $(-)$ indices will be extensively used, referring to tensile and compressive entities, respectively. In this work, the stress split will be performed as in Cervera et al. (1995, 1996) and Faria et al. (1998):

$$\overline{\boldsymbol{\sigma}}^{+} = \sum_{j=1}^{3} < \overline{\sigma}_j > \mathbf{p}_j \otimes \mathbf{p}_j \qquad \text{and} \qquad \overline{\boldsymbol{\sigma}}^{-} = \overline{\boldsymbol{\sigma}} - \overline{\boldsymbol{\sigma}}^{+} \tag{3.2}$$

where $\overline{\sigma}_j$ denotes the *j–th* principal stress value from tensor $\overline{\boldsymbol{\sigma}}$, $\mathbf{p}_j$ represents the unit vector associated with its respective principal direction and the symbol $\otimes$ denotes the tensor product. The symbols $\langle\cdot\rangle$ are the Macaulay brackets ($\langle x\rangle = x$, if $x \geq 0, \langle x\rangle = 0$, if $x < 0$).

Constitutive Equation

The constitutive equation for the damage model is obtained using Coleman's method as:

$$\boldsymbol{\sigma} = \; (1 - d^{+})\, \overline{\boldsymbol{\sigma}}^{+} + (1 - d^{-})\, \overline{\boldsymbol{\sigma}}^{-} \tag{3.3}$$

where we have introduced two internal-like variables, d^{+} and d^{-}, the damage indices under tension and compression, respectively, whose definition and evolution in terms of the real internal variables will be given later.

Characterization of Damage

In order to clearly define concepts such as loading, unloading, or reloading for general 3D stress states, a scalar positive quantity, termed as *normalized equivalent stress*, will be defined. This will permit the comparison of different 3D stress states, even for different degrees of hydration. With such a definition, distinct tridimensional stress states can be mapped to a single *normalized equivalent 1D stress test*, which makes their quantitative comparison possible.

As a consequence of the stress split, two separate equivalent effective stress norms are necessary: a normalized equivalent effective tensile norm τ^+, and a normalized equivalent effective compressive norm τ^-. In the present work they will assume the following form [Cervera et al. 1998]:

$$\tau^{\pm} = \left[\left(\frac{\overline{\boldsymbol{\sigma}}^{\pm}}{f_e^{\pm}} \right) : \mathbf{C}^{\pm} : \left(\frac{\overline{\boldsymbol{\sigma}}^{\pm}}{f_e^{\pm}} \right) \right]^{1/2} = \frac{1}{f_e^{\pm}} \left[\overline{\boldsymbol{\sigma}}^{\pm} : \mathbf{C}^{\pm} : \overline{\boldsymbol{\sigma}}^{\pm} \right]^{1/2} \tag{3.4}$$

where two non-dimensional fourth order metric tensors $\mathbf{C}^{\pm}$ have been introduced. The role of these tensors is to define the shape of the damage bounding surfaces in a normalized effective stress space, as it will be explained below. Note that the two metric tensors can be different for the tensile and compressive norms, $\mathbf{C}^+$ and $\mathbf{C}^-$, respectively.

The normalizing factors $f_e^{\pm}$ represent the values of the tensile f_e^+ and compressive f_e^- uniaxial stresses that define the onset of damage under uniaxial tension and compression, respectively. These values can be taken as proportional to the corresponding peak strengths $f^{\pm}$ as $f_e^- = \lambda_e^- f^-$ and $f_e^+ = \lambda_e^+ f^+$, respectively.

With the above definitions for the equivalent effective stresses, two separated damage criteria, g^+ and g^-, are introduced for tension and compression, respectively:

$$g^{\pm}\left(\tau^{\pm}, r^{\pm}\right) = \tau^{\pm} - r^{\pm} \leq 0 \tag{3.5}$$

Variables r^+ and r^- are normalized internal strain-like variables which can be interpreted as current damage thresholds, in the sense that their values control the size of the (monotonically) expanding damage surfaces. Due to their normalized nature, the initial values are unitary, $r_0^+ = r_0^- = 1$.

This means that the damage criteria are defined in a normalized effective stress space (or in a normalized strain space). In fact, the shape of the damage criteria is defined by the metric tensors $\mathbf{C}^{\pm}$. These tensors must be isotropic and positive

definite, in the form [Cervera et al. 1998]:

$$\mathbf{C}^{\pm} = (1+\gamma^{\pm})\,\mathbf{I} - \gamma^{\pm}\,\mathbf{1}\otimes\mathbf{1} \qquad \text{with} \qquad 0 \le \gamma^{\pm} < 1 \quad (3.6)$$

where $\mathbf{I}$ is the fourth order unit tensor, $\mathbf{1}$ is the second order unit tensor and $\gamma^{\pm}$ is a parameter related to the equibiaxial tensile/compressive strengths. Calling $\rho^{\pm}$ to the ratio between the biaxial and uniaxial strengths, it is

$$\gamma^{\pm} = 1 - \frac{1}{2\,(\rho^{\pm})^2} \quad (3.7)$$

Figures 1 and 2 show 2D representations of the damage criteria for two possible selections of these tensors:

(a) $\gamma^{\pm} = 0$, $\mathbf{C}^{\pm} = \mathbf{I}$ represents a rounded Rankine-type of criterion with $\rho^{\pm} = 1/\sqrt{2} = 0.707$;

(b) $\gamma^{\pm} = 0.622$ represents a much more realistic criterion for concrete with $\rho^{\pm} = 1.15$;

A third possibility is to use:

(c) $\gamma^{\pm} = \nu$, $\mathbf{C}^{\pm} = \overline{\mathbf{D}}^{-1} = (\mathbf{D}/E)^{-1}$represents criteria related to the (normalized) tensile and compressive elastic free energies, but leads to a quite small $\rho^{\pm} = 0.767$.

In this work, we will use option (c): $\mathbf{C}^{\pm} = \overline{\mathbf{D}}^{-1} = (\mathbf{D}/E)^{-1}$. Note that options (a) and (c) are identical if the effect of Poisson's ratio is disregarded.

The evolution (expansion) of the damage bounding surfaces in the normalized space for loading, unloading and reloading conditions is controlled by the Kuhn-Tucker relations and the damage consistency condition, which can be written as

$$\dot{r}^{\pm} \ge 0 \qquad g^{\pm} \le 0 \qquad \dot{r}^{\pm}\,g^{\pm} = 0 \quad (3.8a)$$

$$\dot{r}^{\pm}\,\dot{g}^{\pm} = 0 \quad (3.8b)$$

leading, in view of Eq. (3.5), to the loading condition

$$\dot{r}^{\pm} = \dot{\tau}^{\pm} \quad (3.9)$$

This, in turn, leads to the explicit definition of the current values of the internal variables in the form

$$r^{\pm} = \max\left[r_0^{\pm},\, \max(\tau^{\pm})\right] \quad (3.10)$$

Note that Eq. (3.10) allows to compute the current values for $r^{\pm}$ in terms of the current values of $\tau^{\pm}$, which in turn, depend

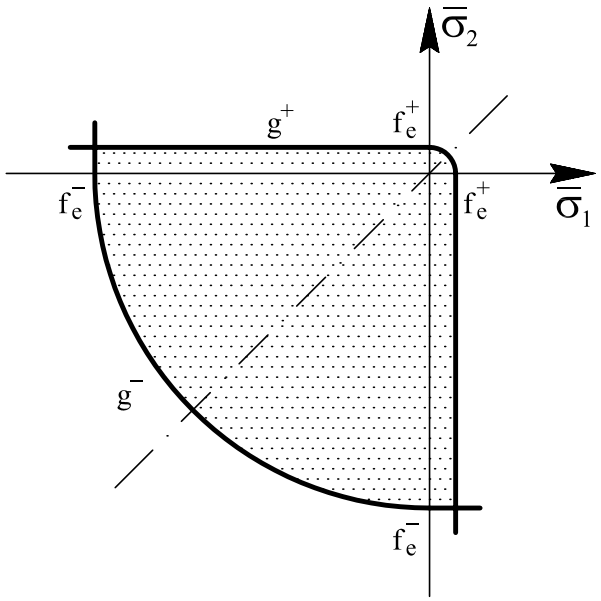

Figure 1 Rankine type of damage criteria

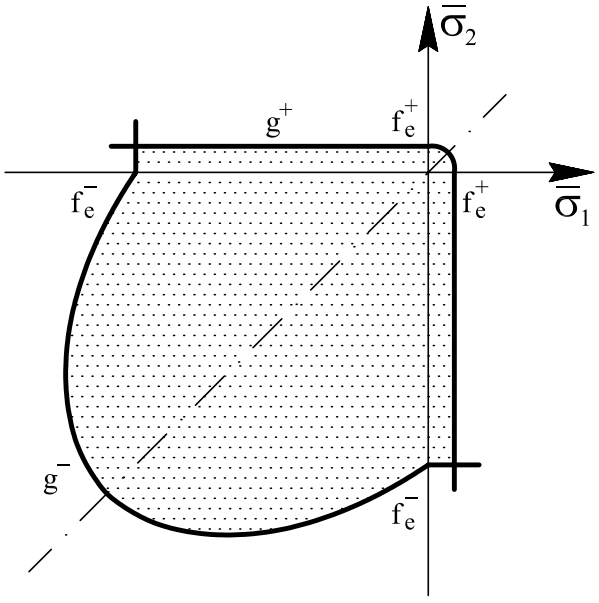

Figure 2 Concrete type of damage criteria

explicitly on the current strains, temperature and degree of aging (see Eqs. (3.1) and (3.4)).

Finally, the damage indices d^+ and d^- are explicitly defined in terms of the corresponding current values of the damage thresholds, so that they are monotonically increasing functions such that $0 \leq d^{\pm}(r^{\pm}) \leq 1$. Let us drop the superindex $(\pm)$ in the following for the sake of brevity, and let us introduce the values $r_e = 1/\lambda_e = f/f_e$, establishing the size of the bounding damage surface for the onset of damage *in the effective stress space*, and $r_p \geq r_e$, establishing the size of the bounding damage surface at peak strength. These two values define the strain-hardening part of the uniaxial stress-strain curve for the material, as it is shown in Figure 3. Note that necessarily $r_p \geq r_e \geq r_0 = 1$. For the limit case $r_p = r_e = r_0 = 1$ the material would exhibit softening immediately after the onset of damage, which is an option often used for tensile strain-softening.

In this work, we will use the functions [Cervera et al. 1998]:

- *parabolic hardening:*

$$d(r) = A_d \frac{r_e}{r} \left(\frac{r-1}{r_p - 1} \right)^2 \qquad r_0 \leq r \leq r_p \qquad (3.11)$$

- *linear or exponential softening:*

$$d(r) = 1 - \frac{r_e}{r} + H_d \left(1 - \frac{r_p}{r} \right) \qquad r_p \leq r \qquad (3.12a)$$

$$d(r) = 1 - \frac{r_e}{r} \exp\left\{ 2H_d \left(\frac{r_p - r}{r_e} \right) \right\} \qquad r_p \leq r \qquad (3.12b)$$

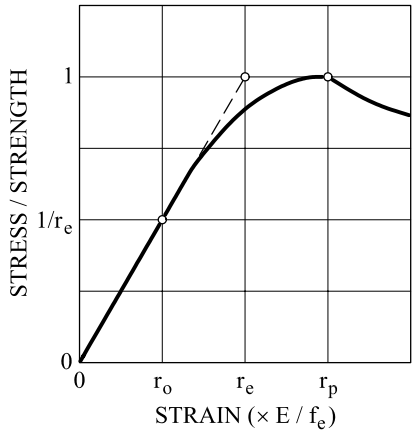

Figure 3 Normalized uniaxial stress-strain curve

where the constants A_d, $H_d \geq 0$ are defined as

$$A_d = \frac{r_p - r_e}{r_e} \tag{3.13a}$$

$$\frac{1}{H_d} = 2\left(\frac{EG_f}{f^2}\frac{1}{l_{\text{ch}}} - \frac{1}{2}\frac{r_p}{r_e} - \overline{A}_d\right) \tag{3.13b}$$

where $\overline{A}_d = A_d\,(r_p^3 - 3r_p + 2/3)\,/\,6\,r_e\,(r_p - 1)^2$. In Eq. (3.13b) the fracture energies (under tension and compression) of the material G_f and the characteristic length l_{ch} have been introduced to ensure mesh-size objective results (see below).

Rate dependent damage

There is a strong coupling between nonlinear rate-sensitivity in concrete (and other geomaterials) and damage growth. Therefore, it is natural to develop a rate dependent constitutive model within the framework of CDMT, evolving from the above presented rate independent damage model, and which accounts for strain rate dependency via the damage evolution laws.

To this end, let us consider a viscous regularization of the rate-independent damage thresholds evolution laws defined by Eqs. (3.9), so that these are replaced by [Cervera et al. 1996]:

$$\dot{r}^{\pm} = \frac{\phi^{\pm}(\tau^{\pm} - r^{\pm})}{\vartheta^{\pm}} \geq 0 \tag{3.14}$$

where $\phi^{\pm}(\cdot)$ are scalar functions called the viscous damage threshold flow functions; $\vartheta^{\pm}$ are the retardation times for damage. Note that the modification of the evolution laws only affects the integration of the damage thresholds (r^+ and r^-), but not the damage variables (d^+ and d^-) themselves. These are still obtained in a closed form, through the explicit definition of the functions $d^+(r^+)$ and $d^-(r^-)$. Additionally, it is worth to remark that Eqs. (3.14) must guarantee monotonic increasing of the damage thresholds, and, therefore, also of the damage indices ($\dot{d}^+ \geq 0$ and $\dot{d}^- \geq 0$).

It must be noted that the definition of the evolution law (2.15) replaces the Kuhn-Tucker and consistency conditions, Eqs. (3.8a) and (3.8b), of the rate independent model.

The viscous threshold damage flow functions may assume the following form:

$$\phi^{\pm}(\tau^{\pm} - r^{\pm}) = r_0{}^{\pm}\left\langle\frac{\tau^{\pm} - r^{\pm}}{r_0{}^{\pm}}\right\rangle^{a^{\pm}} \tag{3.15}$$

Note that $a^{\pm}$ are positive exponents, also supposed to be material properties. The determination of these exponents, as well as that of the retardation times is done by means of uniaxial tensile and compressive tests. Note that different values can be attributed to the tensile and compressive parameters and exponents, and this will allow to account for different rate sensitivities under tensile and compressive loading. Note that this definition ensures that expression (3.14) is dimensionally correct. This is necessary for ϑ to retain its physical meaning of retardation time for the evolution of damage.

The reasoning behind the above laws is analogous to the classical Perzyna viscoplastic regularization often used in the framework of Computational Plasticity. It can be seen that this assumed rate dependent formulation is a general form for the damage threshold and damage evolution, so that for a very small value of the retardation damage parameter, the rate-independent (or inviscid) damage evolution law is recovered, while for an infinite value of ϑ, evolution of the damage variables is prevented, thus rendering an instantaneously elastic response.

The rate-dependent model can also be written in a Duvaut-Lions format, as

$$\dot{r} = \frac{\phi\,(r_\infty - r)}{\vartheta} \geq 0 \tag{3.16}$$

where r_∞ is the value of the damage threshold corresponding to the current value of τ as $t/\vartheta \to \infty$. As the rate-dependent (viscous) model relaxes to the rate-independent (inviscid) solution, it is obvious that in the inviscid limit, satisfaction of the consistency condition ensures that $r_\infty = \tau$. Therefore, Ecs. (3.14) and (3.16) are completely equivalent.

Thermodynamic Framework

Let us define the elastic free energies associated with the tensile and compressive effective stresses in the form

$$W_e^{\pm} = W_e^{\pm}(\boldsymbol{\varepsilon}) = \frac{1}{2}\,\overline{\boldsymbol{\sigma}}^{\pm} : \mathbf{D}^{-1} : \overline{\boldsymbol{\sigma}} \tag{3.17}$$

where the superindex $(\pm)$ may mean tension or compression, as convenient. Some algebra is needed to show that $W_e^{\pm} \geq 0$.

The mechanical free energy term for the damage model is defined by combining these elements in the form:

$$\begin{aligned} W &= W(\boldsymbol{\varepsilon}, d^+, d^-) \\ &= W^+(\boldsymbol{\varepsilon}, d^+) + W^-(\boldsymbol{\varepsilon}, d^-) \\ &= (1-d^+)W_e^+(\boldsymbol{\varepsilon}) + (1-d^-)W_e^-(\boldsymbol{\varepsilon}) \end{aligned} \tag{3.18}$$

where d^+ and d^-, the damage indices under tension and compression, respectively. Recalling that $0 \leq d^+, d^- \leq 1$, it can be shown that $W \geq 0$ [Faria et al. 1998].

The constitutive equation for the damage model is obtained using Coleman's method as:

$$\boldsymbol{\sigma} = \partial_{\varepsilon} W = (1-d^+)\,\overline{\boldsymbol{\sigma}}^+ + (1-d^-)\,\overline{\boldsymbol{\sigma}}^- \tag{3.19}$$

The mechanical dissipation can be expressed as

$$\dot{D}_{\text{mech}} = W_e^+ \dot{d}^+ + W_e^- \dot{d}^- \geq 0 \tag{3.20}$$

provided that the damage indices increase monotonically, that is, $\dot{d}^+, \dot{d}^- \geq 0$.

Softening behaviour

Let us now prove that Eq. (3.13b) expresses the correct dependence on the characteristic length. Consider an experiment in which the load increases *monotonically* and *quasi-statically* from an initial unstressed state to another in which full degradation takes place. For the sake of simplicity, we will consider damage only in tension or in compression, but not both. The extension to the general case is straight-forward. Therefor, dropping the superindex $(\pm)$ and using the rate independent version of the model, the specific energy dissipated in the process is:

$$D_{\text{mech}} = \int_{t=0}^{t=\infty} \dot{D}_{\text{mech}}\, dt \tag{3.21a}$$

$$= \int_{t=0}^{t=\infty} W_e\ \dot{d}\, dt \tag{3.21b}$$

$$= \int_{r=r_0}^{r=\infty} \frac{f_e^2}{2E}\, r^2 d'\, dr \tag{3.21c}$$

where we have used Eqs. (3.20), (3.17), (3.1), (3.4), (3.10) and the rate of damage can be expressed as $\dot{d} = d'\,\dot{r}$.

Let us consider the *parabolic hardening* and *linear softening* laws from Eqs. (3.11) and (3.12a). We can write (see also Chapter 2):

$$
\begin{aligned}
D_{\text{mech}} &= \int_{r=r_0}^{r=\infty} \frac{f_e^2}{2E} r^2 d'\, dr && \text{(3.22a)}\\
&= \int_{r=r_0}^{r=r_p} \frac{f_e^2}{2E} r^2 d'\, dr + \int_{r=r_p}^{r=r_u} \frac{f_e^2}{2E} r^2 d'\, dr && \text{(3.22b)}\\
&= \frac{f_e^2}{2E}\left[\frac{A_d}{3r_e}\frac{(r_p^3 - 3r_p + 2/3)}{(r_p-1)^2} + \right. && \text{(3.22c)}\\
&\qquad\qquad \left. + r_e\left(r_p - \frac{1}{H_d}\right)\right] && \text{(3.22d)}\\
&= \frac{f_e^2}{E} r_e^2 \left[\overline{A}_d + \frac{1}{2}\frac{r_p}{r_e} - \frac{1}{2H_d}\right] && \text{(3.22e)}\\
&= \frac{f^2}{E}\left[\overline{A}_d + \frac{1}{2}\frac{r_p}{r_e} - \frac{1}{2H_d}\right] && \text{(3.22f)}
\end{aligned}
$$

where $r_e = f/f_e$, $r_u = r_p + (r_e/H)$ and $\overline{A}_d = A_d\,(r_p^3 - 3r_p + 2/3)\,/\,6\,r_e\,(r_p-1)^2$. Now, equating $D_{\text{mech}} = G_f\,/l_{\text{ch}}$, we have

$$
\begin{aligned}
\frac{1}{H_d} &= 2\left(\frac{EG_f}{f^2}\frac{1}{l_{\text{ch}}} - \frac{1}{2}\frac{r_p}{r_e} - \overline{A}_d\right) && \text{(3.23a)}\\
&= \frac{r_e^2}{\overline{H}\,l_{\text{ch}}} - \frac{1}{2}\frac{r_p}{r_e} - \overline{A}_d && \text{(3.23b)}
\end{aligned}
$$

where $\overline{H} = (f_e)^2/\,2EG_f$ depends only on the material properties.

Now, considering the *parabolic hardening* and *exponential softening* laws from Eqs. (3.11) and (3.12b), we can write

$$
\begin{aligned}
D_{\text{mech}} &= \int_{r=r_0}^{r=\infty} \frac{f_e^2}{2E} r^2 d'\, dr && \text{(3.24a)}\\
&= \int_{r=r_0}^{r=r_p} \frac{f_e^2}{2E} r^2 d'\, dr + \int_{r=r_p}^{r=\infty} \frac{f_e^2}{2E} r^2 d'\, dr && \text{(3.24b)}\\
&= \frac{f_e^2}{2E}\left[\frac{A_d}{3r_e}\frac{(r_p^3 - 3r_p + 2/3)}{(r_p-1)^2} + \right. && \text{(3.24c)}\\
&\qquad\qquad \left. + r_e\left(r_p - \frac{1}{H_d}\right)\right] && \text{(3.24d)}\\
&= \frac{f_e^2}{E} r_e^2 \left[\overline{A}_d + \frac{1}{2}\frac{r_p}{r_e} - \frac{1}{2H_d}\right] && \text{(3.24e)}\\
&= \frac{f^2}{E}\left[\overline{A}_d + \frac{1}{2}\frac{r_p}{r_e} - \frac{1}{2H_d}\right] && \text{(3.24f)}
\end{aligned}
$$

Thanks to the selection of the format for the softening laws, this result is exactly identical to the one for the linear case.

Therefore, we have the same expression for the softening modulus H_d in both cases, Eqs. (3.23a) or (3.23b).

Note that for the limit case $r_0 = r_e = r_p = 1$, Eq. (3.13a) yields $A_d = 0$ and then Eqs. (3.23a) and (3.23b) reduce to

$$H_d = \frac{\overline{H}\, l_{\rm ch}}{1 - \overline{H}\, l_{\rm ch}} \tag{3.25}$$

a well-known result for linear and exponential softening (see Chapter 2 and Cervera et al. 1995, 1996).

Integration of the internal variables

A numerical algorithm needs to be implemented for the time integration of the damage constitutive equations presented in the previous sections. In the following this algorithm is presented, in a strain–driven form which leads to an almost closed–form algorithm to integrate the stress tensor in time. This is most appropriate within the context of the application of the finite element method.

Each time step begins at time t_n with all state variables known and it ends at time t_{n+1} with the state variables updated according to the given total strain tensor $\boldsymbol{\epsilon}$. The time step size is $\Delta t = t_{n+1} - t_n$.

For the rate independent model, Eq. (3.10) allows to compute the current values for $r^{\pm}_{n+1}$ in terms of the current values of $\tau^{\pm}_{n+1}$, which in turn, depend explicitly on the current strains $\boldsymbol{\epsilon}_{n+1}$(see Eqs. (3.1) and (3.4)). After this, the damage indices $d^{\pm}_{n+1}$ are explicitly computed in terms of the corresponding current values of the damage thresholds, using the appropriate expressions, Eqs. (3.12a) or (3.12b).

For the rate dependent model, the only difference is the updating of the damage thresholds when evolution of the damage occurs, that is, upon loading conditions. Let us drop the superindex $(\pm)$ in the following for the sake of brevity. The damage thresholds may be evaluated using a generalized midpoint rule to integrate Eq. (3.14), i.e.,

$$r_{n+1} \;=\; r_n + \frac{\Delta t}{\vartheta}\, \phi(\tau_\alpha - r_\alpha) \tag{3.26}$$

where τ_α and r_α are defined by:

$$\tau_\alpha \quad = \quad (1-\alpha)\, \tau_n + \alpha\, \tau_{n+1} \tag{3.27a}$$

$$r_\alpha \;=\; (1-\alpha)\, r_n + \alpha\, r_{n+1} \tag{3.27b}$$

For the sake of shortness, we can write Eq. (3.26) as:

$$r_{n+1} \;=\; r_n + \Delta r_{n+1} \;=\; r_n + \frac{\Delta t}{\vartheta}\,\phi_\alpha \tag{3.28}$$

where ϕ_α represents the value of function ϕ evaluated at time α, that is

$$\begin{aligned} \phi_\alpha \;&=\; \phi\,(\tau_\alpha - r_\alpha) && (3.29a)\\ &=\; \phi\,[(1-\alpha)(\tau_n - r_n) + \alpha(\tau_{n+1} - r_{n+1})] && (3.29b) \end{aligned}$$

Note that for $\alpha = 1$ Eq. (3.28) corresponds to a backward-Euler difference scheme. It is easy to show that the algorithm of Eq. (3.28) is unconditionally stable for $\alpha \geq 0.5$ and second order accurate only for $\alpha = 0.5$ (Crank-Nicholson or trapezoidal rule), which allows the use of larger time step sizes for rate-dependent analysis.

It is obvious that the explicit determination of r_{n+1} is possible only for small integer values of the exponent a in Eq. (3.15), as the cases $a = 1, 2, 3$ lead to linear, quadratic and cubic expressions for Eq. (3.28), respectively. For instance, for $a = 1$ it is

$$\Delta r_{n+1} \;= \frac{\frac{\Delta t}{\vartheta}\,[(1-\alpha)(\tau_n - r_n) + \alpha(\tau_{n+1} - r_{n+1})]}{1 + \alpha\frac{\Delta t}{\vartheta}} \tag{3.30}$$

In the general case, Eq. (3.28) may be solved by the iterative Newton-Raphson method, which ensures a fast rate of convergence. To this purpose, Eq. (3.28) may be rewritten as:

$$f(r_{n+1}) \;=\; 0 \;=\; -r_{n+1} \;+\; r_n + \frac{\Delta t}{\vartheta}\,\phi_\alpha \tag{3.31}$$

so that the problem is now to find the root of Eq. (3.31) by an iterative Newton-Raphson procedure given by:

$$r^{i+1}_{n+1} \;=\; r^{i}_{n+1} - \frac{f(r^{i}_{n+1})}{f'(r^{i}_{n+1})} \tag{3.32}$$

where r^{i+1}_{n+1} indicates an improved approximation to the exact root obtained from the previous r^{i+1}_{n+1} approximation and f' is the first derivative of function f with respect to r_{n+1}. This leads to the iterative update of the increment Δr_{n+1} in the form

$$\Delta r^{i+1}_{n+1} \;= \frac{\frac{\Delta t}{\vartheta}\left[\phi_\alpha + \alpha\,\phi'_\alpha\,\Delta r^{i}_{n+1}\right]}{1 + \alpha\frac{\Delta t}{\vartheta}} \tag{3.33}$$

where ϕ'_α represents the value of the derivative of function ϕ evaluated at time α. The iteration procedure starts for $i = 0$ with $\Delta r^0_{n+1} = 0$ and finishes when a preselected convergence criterion is satisfied.

A useful alternative to the use of the Newton-Raphson procedure is the linealization of Ec. (3.29a) in the form

$$\begin{aligned} \phi_\alpha &\simeq \phi_n + \phi'_n \cdot [(\tau_\alpha - r_\alpha) - (\tau_n - r_n)] && \text{(3.34a)} \\ &= \phi_n + \alpha\, \phi'_n \cdot [(\tau_{n+1} - \tau_n) - (r_{n+1} - r_n)] && \text{(3.34b)} \end{aligned}$$

This leads to an explicit update of the increment Δr_{n+1} in the form

$$\Delta r_{n+1} = \frac{\frac{\Delta t}{\vartheta}\,[\phi_n + \alpha\, \phi'_n \cdot (\tau_{n+1} - \tau_n)]}{1 + \alpha \frac{\Delta t}{\vartheta}} \qquad (3.35)$$

Note that in Eq. (3.26) the condition to update the damage threshold is $\tau_\alpha > r_\alpha$. However, r_α cannot be computed before a new value for r_{n+1} is found. Therefore, the previous condition is changed in the algorithm by an alternative check, $\tau_\alpha > r_n$. Consequently, once a converged value for r_{n+1} has been computed according to the described procedure, Eq. (3.27b) is used to evaluate the corresponding r_α value. Then a check is performed to ensure that the condition $\tau_\alpha > r_\alpha$ is satisfied. Otherwise, there is no evolution of damage in the time step and, therefore, $r_{n+1} = r_n$.

Tangent operator

Differentiating Eq.(3.3) with respect to time, we obtain

$$\dot{\boldsymbol{\sigma}} = \; (1 - d^+)\, \dot{\overline{\boldsymbol{\sigma}}}^+ + (1 - d^-)\, \dot{\overline{\boldsymbol{\sigma}}}^- - \dot{d}^+\, \overline{\boldsymbol{\sigma}}^+ - \dot{d}^-\, \overline{\boldsymbol{\sigma}}^- \qquad (3.36)$$

Also, differentiating Eq.(3.1) with respect to time, we have

$$\dot{\overline{\boldsymbol{\sigma}}} = \mathbf{D} : \dot{\boldsymbol{\varepsilon}} \qquad (3.37)$$

Despite the simplicity of the stress split postulated in Eq. (3.2), which expresses $\overline{\boldsymbol{\sigma}}^\pm$ in terms of the eigenvalues and eigenvectors of $\overline{\boldsymbol{\sigma}}$, quite more involved operations are required to express $\dot{\overline{\boldsymbol{\sigma}}}^\pm$ in terms of $\dot{\overline{\boldsymbol{\sigma}}}$. It can be shown that the appropriate expressions are [Faria et al. 2001]

$$\begin{aligned} \dot{\overline{\boldsymbol{\sigma}}}^+ &= \mathbf{P} : \dot{\overline{\boldsymbol{\sigma}}} \qquad = \mathbf{P} : \mathbf{D} : \dot{\boldsymbol{\varepsilon}} && \text{(3.38a)} \\ \dot{\overline{\boldsymbol{\sigma}}}^- &= (\mathbf{I} - \mathbf{P}) : \dot{\overline{\boldsymbol{\sigma}}} \; = \; (\mathbf{I} - \mathbf{P}) : \mathbf{D} : \dot{\boldsymbol{\varepsilon}} && \text{(3.38b)} \end{aligned}$$

where the projection operator $\mathbf{P}$ is

$$\mathbf{P} = \sum_{i=1}^{3} H\left(\overline{\sigma}_i\right) \mathbf{P}^{ii} \otimes \mathbf{P}^{ii} + 2 \sum_{\substack{i,j=1 \\ j>i}}^{3} \frac{\langle \overline{\sigma}_i \rangle - \langle \overline{\sigma}_j \rangle}{\overline{\sigma}_i - \overline{\sigma}_j} \mathbf{P}^{ij} \otimes \mathbf{P}^{ij} \quad (3.39)$$

where $H\left(\cdot\right)$ is the Heaviside function, $\langle \cdot \rangle$ are the Macaulay brackets and

$$\mathbf{P}^{ij} = \mathbf{P}^{ji} = \frac{1}{2}\left(\mathbf{p}_i \otimes \mathbf{p}_j + \mathbf{p}_j \otimes \mathbf{p}_i\right) = \mathrm{symm}\left(\mathbf{p}_i \otimes \mathbf{p}_j\right) \quad (3.40)$$

On the other hand, the time derivative of the damage indices is

$$\dot{d}^{\pm} = \left(d^{\pm}\right)' \dot{r}^{\pm} \quad (3.41)$$

where the first derivative term can be obtained from Eqs.(3.12a)-(3.12b). On loading, consistency requires that $\dot{r}^{\pm} = \dot{\tau}^{\pm}$, and therefore, differentiating Eq. (3.4), we can write

$$\begin{aligned} \dot{r}^{+} &= \dot{\tau}^{+} \\ &= \frac{1}{\left(f_e^{+}\right)^2} \frac{1}{\tau^{+}} \left[\overline{\boldsymbol{\sigma}}^{+} : \mathbf{C}^{+} : \dot{\overline{\boldsymbol{\sigma}}}^{+} \right] \\ &= \frac{1}{\left(f_e^{+}\right)^2} \frac{1}{\tau^{+}} \left[\overline{\boldsymbol{\sigma}}^{+} : \mathbf{C}^{+} : \mathbf{P} : \mathbf{D} : \dot{\boldsymbol{\varepsilon}} \right] \qquad (3.42a) \\ \dot{r}^{-} &= \dot{\tau}^{-} \\ &= \frac{1}{\left(f_e^{-}\right)^2} \frac{1}{\tau^{-}} \left[\overline{\boldsymbol{\sigma}}^{-} : \mathbf{C}^{-} : \dot{\overline{\boldsymbol{\sigma}}}^{-} \right] \\ &= \frac{1}{\left(f_e^{-}\right)^2} \frac{1}{\tau^{-}} \left[\overline{\boldsymbol{\sigma}}^{-} : \mathbf{C}^{-} : (\mathbf{I} - \mathbf{P}) : \mathbf{D} : \dot{\boldsymbol{\varepsilon}} \right] \qquad (3.42b) \end{aligned}$$

On unloading, it is $\dot{r}^{\pm} = 0$. Substituting these results in Eq. (3.41), and the result in Eq. (3.36), jointly with Eqs. (3.38a) and (3.38b), yields the desired expression

$$\dot{\boldsymbol{\sigma}} = \mathbf{D}^{\tan} : \dot{\boldsymbol{\varepsilon}} \quad (3.43)$$

with

$$\begin{aligned} \mathbf{D}^{\tan} = & \left[\left\{ (1 - d^{+})\, \mathbf{I} - h^{+} \left(\overline{\boldsymbol{\sigma}}^{+} \otimes \overline{\boldsymbol{\sigma}}^{+} \right) : \mathbf{C}^{+} \right\} : \mathbf{P} + \right. \qquad (3.44) \\ & \left. + \left\{ (1 - d^{-})\, \mathbf{I} - h^{-} \left(\overline{\boldsymbol{\sigma}}^{-} \otimes \overline{\boldsymbol{\sigma}}^{-} \right) : \mathbf{C}^{-} \right\} : (\mathbf{I} - \mathbf{P}) \right] : \mathbf{D} \end{aligned}$$

where the coefficients $h^{\pm}$ are

$$h^{\pm} = \begin{cases} \dfrac{1}{\left(f_e^{\pm}\right)^2} \dfrac{\left(d^{\pm}\right)'}{\tau^{\pm}} & \text{for loaging} \\ \\ 0 & \text{for unloading} \end{cases} \quad (3.45)$$

Note that this tensor operator is, in general, unsymmetrical.. However, for the particular choice of *associative damage*, $\mathbf{C}^{\pm} = \overline{\mathbf{D}}^{-1} = \left(\mathbf{D}/E\right)^{-1}$, it is symmetric.

Rate dependent damage

In the case of rate dependent damage the determination of $\dot{r}^{\pm}$ comes from differentiating Eq. (3.28) with respect to time, to yield:

$$\dot{r}^{\pm} = \frac{\alpha \frac{\Delta t}{\vartheta} \left(\phi_{\alpha}^{\pm}\right)'}{1 + \alpha \frac{\Delta t}{\vartheta} \left(\phi_{\alpha}^{\pm}\right)'} \dot{\tau}^{\pm} \tag{3.46}$$

where $\left(\phi_{\alpha}^{\pm}\right)'$ represents the value of the derivative of function $\phi^{\pm}$ evaluated at time α. Note that when using the approximation of Ec. (3.34a), $\left(\phi_{\alpha}^{\pm}\right)' \simeq \left(\phi_{n}^{\pm}\right)'$. Comparing Eqs. (3.42a)-(3.42b) and (3.46), it is obvious that the tangent operator for the rate dependent damage case has the same expression of Eq. (3.44), with the coefficients $h^{\pm}$ given by

$$h^{\pm} = \begin{cases} \dfrac{\alpha \frac{\Delta t}{\vartheta} \left(\phi_{\alpha}^{\pm}\right)'}{1 + \alpha \frac{\Delta t}{\vartheta} \left(\phi_{\alpha}^{\pm}\right)'} \dfrac{1}{\left(f_{e}^{\pm}\right)^2} \dfrac{\left(d^{\pm}\right)'}{\tau^{\pm}} & \text{for loading} \\ 0 & \text{for unloading} \end{cases} \tag{3.47}$$

Note that for large values of $\Delta t/\vartheta$ the rate independent case is recovered.

Coupling with visco-elasticity

Let us now consider the coupling of the viscoelastic model described in Chapter 1 with the damage model described above. The basic hypothesis is that the stress sustained by the Maxwell chain is the effective (undamaged) stress, rather than the total stress (see Figure 4). This idea is based on the CDMT concept that it is the effective stress the one acting on the effective (undamaged) solid concrete, while the total stress acts on the whole (damaged) solid [Cervera et al. 1998].

Let us begin by defining the effective stresses and the elastic strains for one element of the Maxwell chain as:

$$\overline{\boldsymbol{\sigma}}^{i} = \xi^{i} \mathbf{D} : (\boldsymbol{\varepsilon} - \boldsymbol{\varepsilon}^{i}) \tag{3.48}$$

with $\xi^{i} = E^{i}/E$ being the participation factor of $i-th$ element, and $\boldsymbol{\varepsilon}^{i}$ being the viscous strains in each Maxwell element, with

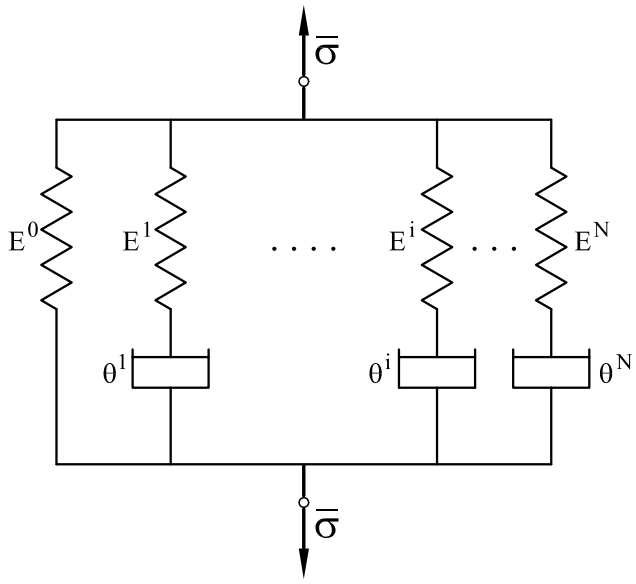

Figure 4 Maxwell chain subjected to effective stress

the evolution law:

$$\dot{\boldsymbol{\varepsilon}}^i = \frac{1}{\vartheta^i}\,(\boldsymbol{\varepsilon} - \boldsymbol{\varepsilon}^i) \qquad \text{for} \quad i = 0, 1, ..., N \tag{3.49}$$

where ϑ^i are the relaxation times of the corresponding dashpots. Let us also define the stress split for each element, as

$$\overline{\boldsymbol{\sigma}}^{i+} = \sum_{j=1}^{3} < \overline{\sigma}_j^i > \mathbf{p}_j^i \otimes \mathbf{p}_j^i \qquad \text{and} \qquad \overline{\boldsymbol{\sigma}}^{i-} = \overline{\boldsymbol{\sigma}}^i - \overline{\boldsymbol{\sigma}}^{i+} \tag{3.50}$$

where $\overline{\sigma}_j^i$ denotes the *j–th* principal stress value from tensor $\overline{\boldsymbol{\sigma}}^i$, $\mathbf{p}_j^i$ represents the unit vector associated with its respective principal direction and the symbol $\otimes$ denotes the tensor product.

Let us define the elastic free energy associated with the tensile and compressive effective stresses for each element in the form

$$W_e^{i+} = W_e^{i+}(\boldsymbol{\varepsilon}, \boldsymbol{\varepsilon}^i) = \frac{1}{2}\,\overline{\boldsymbol{\sigma}}^{i+} : (\xi^i\,\mathbf{D})^{-1} : \overline{\boldsymbol{\sigma}}^{i+} \tag{3.51a}$$

$$W_e^{i-} = W_e^{i-}(\boldsymbol{\varepsilon}, \boldsymbol{\varepsilon}^i) = \frac{1}{2}\,\overline{\boldsymbol{\sigma}}^{i-} : (\xi^i\,\mathbf{D})^{-1} : \overline{\boldsymbol{\sigma}}^{i-} \tag{3.51b}$$

The total elastic free energy associated to the Maxwell chain is obtained by adding the contributions of the elements

$$W_e = W_e(\boldsymbol{\varepsilon}, \boldsymbol{\varepsilon}^i) \tag{3.52a}$$

$$= W_e^{+}(\boldsymbol{\varepsilon}, \boldsymbol{\varepsilon}^i) + W_e^{-}(\boldsymbol{\varepsilon}, \boldsymbol{\varepsilon}^i) \tag{3.52b}$$

$$= \sum_{i=0}^{N} W_e^{i+}(\boldsymbol{\varepsilon}, \boldsymbol{\varepsilon}^i) + \sum_{i=0}^{N} W_e^{i-}(\boldsymbol{\varepsilon}, \boldsymbol{\varepsilon}^i) \tag{3.52c}$$

Introducing the damage indices under tension and compression d^+ and d^-, respectively, the mechanical free energy is defined by combining previously defined items in the form:

$$\begin{aligned} W &= W(\boldsymbol{\varepsilon}, \boldsymbol{\varepsilon}^i, d^+, d^-) && (3.53a)\\ &= W^+(\boldsymbol{\varepsilon}, \boldsymbol{\varepsilon}^i, d^+, d^-) + W^-(\boldsymbol{\varepsilon}, \boldsymbol{\varepsilon}^i, d^+, d^-) && (3.53b)\\ &= (1-d^+)\, W_e^+(\boldsymbol{\varepsilon}, \boldsymbol{\varepsilon}^i) + (1-d^-)\, W_e^-(\boldsymbol{\varepsilon}, \boldsymbol{\varepsilon}^i) && (3.53c) \end{aligned}$$

It can be shown that $W \geq 0$.

The stresses are obtained as:

$$\begin{aligned} \boldsymbol{\sigma} &= \partial_\varepsilon W && (3.54a)\\ &= \partial_\varepsilon W^+ + \partial_\varepsilon W^- && (3.54b)\\ &= (1-d^+) \sum_{i=0}^{N} \overline{\boldsymbol{\sigma}}^{i+} + (1-d^-) \sum_{i=0}^{N} \overline{\boldsymbol{\sigma}}^{i-} && (3.54c)\\ &= (1-d^+)\, \overline{\boldsymbol{\sigma}}^+ + (1-d^-)\, \overline{\boldsymbol{\sigma}}^- && (3.54d) \end{aligned}$$

so that the same final form as in Eq. (3.3) is obtained for the damage model.

The definition of the damage surfaces and the evolution of the damage indices and thresholds can be done in terms of the total tensile and compressive parts of the effective stress, $\overline{\boldsymbol{\sigma}}^+$ and $\overline{\boldsymbol{\sigma}}^-$, as explained previously.

The mechanical dissipation can be split into its viscoelastic and damage parts, in the form:

$$\mathcal{D}_{\text{mech}} = \sum_{i=0}^{N} \frac{2}{\vartheta^i} W_e^i + W_e^+ \dot{d}^+ + W_e^- \dot{d}^- \geq 0 \qquad (3.55)$$

Tangent operator

Following the same arguments outlined in Chapter 2, the rate form of the viscoelasticity damage model is written as:

$$\dot{\boldsymbol{\sigma}} = \mathbf{D}^{\tan} : \dot{\boldsymbol{\varepsilon}} \qquad (3.56)$$

with

$$\begin{aligned} \mathbf{D}^{\tan} = {} & \big[\{(1-d^+)\, \mathbf{I} - h^+ \, (\overline{\boldsymbol{\sigma}}^+ \otimes \overline{\boldsymbol{\sigma}}^+) : \mathbf{C}^+\} : \mathbf{P} + \\ & + \{(1-d^-)\, \mathbf{I} - h^- \, (\overline{\boldsymbol{\sigma}}^- \otimes \overline{\boldsymbol{\sigma}}^-) : \mathbf{C}^-\} : (\mathbf{I} - \mathbf{P}) \big] : \mathbf{D}^{\text{visc}} \end{aligned} \qquad (3.57)$$

where the coefficients $h^\pm$ are those given in Eqs. (3.45) or (3.47), depending on the case, and $\mathbf{D}^{\text{visc}}$ is that of Eq. (1.18)

$$\mathbf{D}^{\text{visc}} = \left[\sum_{i=0}^{N} \xi^i e^{-\frac{\Delta t}{\vartheta^i}} \right] \mathbf{D} \qquad (3.58)$$

As explained in Chapter 2, this expression neglects the unsymmetrical coupling terms between viscoelasticity and damage. Therefore, it is only and approximate tangent operator, and it will not render quadratic convergence when used in a Newton-Raphson iterative scheme.

Numerical examples

In order to verify the performance of the constitutive damage model described above, some numerical examples are presented.

These examples focus on the influence of the parameters defining the model on the obtained behaviour. The parameters needed to define the model are summarized in Table 3.1. In this Table, reference to the different material properties is made both in the notation used in the text and with the names of the variables that the finite element program COMET [Cervera et al. 2002] uses to denote the corresponding parameters.

Name	**Text**	**Variable**
Young's modulus	E	`YOUNG`
Poisson's ratio	ν	`POISS`
Tensile strength	f^+	`STREN`
Hardening/Softening law	$-$	`ILAWT`
Linear hardening parameter	$-$	`HFACT`
Tensile fracture energy	G_f^+	`GFRAC`
Retardation time for tensile damage	ϑ^+	`RETAT`
Compr./Tensile strengths ratio	$f^- \,/\, f^+$	`RACTS`
Compr. damage thres./strength ratio	$f_e^- \,/\, f^-$	`CDAMG`
Compressive fracture energy	G_f^-	`GFCOM`
Strain at peak compressive strength	ϵ^-	`EPSUC`
Relaxation time for compr. damage	ϑ^-	`RETAC`
Number of Maxwell chains	N	`NMAXW`
Elasticity modulus ratio for chain i	ξ^i	`ELASi`
Retardation time for chain i	ϑ^i	`RETAi`

Table 3.1 Parameters used in the model

To conduct the desired tests on the numerical integration of the constitutive model a finite element model must be defined, together with the appropriate boundary and loading conditions.

To this end, a FE mesh consisting of a single four-noded element of 1×1 m in the $x - y$ plane, simply (isostatically) supported is used. Plane strain conditions are assumed in the z-direction. The element is loaded in x-direction by imposing a prescribed displacement that follows the cyclic time history shown in Figure 5. A constant time step size of $\Delta t = 10$ s was used to perform the analyses.

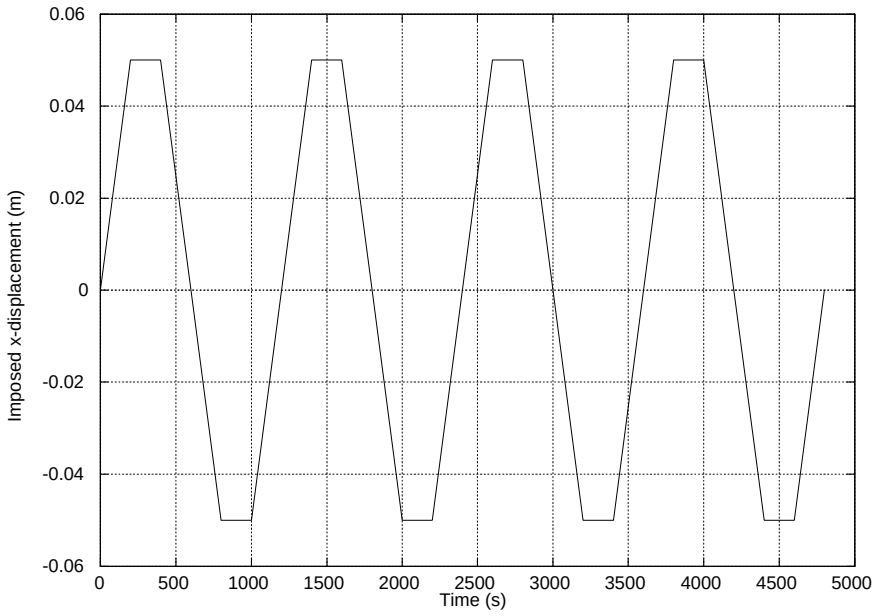

Figure 5 Cyclic load

Rate dependency

Two different cases are defined to study the influence of the retardation time for damage. The values used in the models are showed in Table 3.2. Two different values of the retardation time for damage are used in each case. All units are in the SI system. Note that in Case 1 the ratio $f^- / f^+ = 1$, while in Case 2 $f^- / f^+ = 10$.

Variable	**Case 1**	**Case 2**
YOUNG	100 000	100 000
POISS	0.3	0.3
STREN	2 500	2 500
ILAWT	0	0
HFACT	0.2	0.2
RETAT	0 / 500	0 / 500
RACTS	1	10
CDAMG	1	1
RETAC	RETAT	RETAT

Table 3.2 Values of material properties

Results for Case 1 are shown in Figures 6 and 7. Figure 6 shows the stress evolution in time, compared with a purely elastic behaviour. Figure 7 shows the corresponding stress *versus* strain curve for the rate independent case. It can be observed that damage occurs symmetrically in tension and compression, as the corresponding strengths are equal. Also, in the first cycle, the original undamaged stiffness is recovered upon loading reversal.

Results for Case 2 are shown in Figures 8 and 9. Figure 8 shows the stress evolution in time, compared with a purely elastic behaviour. Figure 9 shows the corresponding stress *versus* strain curve for the rate independent case. It can be observed that damage occurs only in tension, as the compressive strength is not reached. Note how the undamaged stiffness is recovered upon loading reversal.

Softening behaviour

Two more cases are defined to study the influence of softening behavior. The values used in the models are showed in Table 3.3. Two different values of the retardation time for damage are used in each case. All units are in the SI system. Note that in both cases the ratio $f^- / f^+ = 1$, and the ratio $f_e^- / f^- = 0.5$.

Variable	Case 3	Case 4
YOUNG	100 000	100 000
POISS	0.3	0.3
STREN	2 500	2 500
ILAWT	1	1
GFRAC	156.25	156.25
RETAT	0	500
RACTS	1	1
CDAMG	0.5	0.5
GFCOM	GFRAC	GFRAC
RETAC	RETAT	RETAT

Table 3.3 Values of material properties

Results for Case 3 are shown in Figures 10 and 11. Figure 10 shows the stress evolution in time, compared with a purely elastic behaviour. Figure 11 shows the corresponding stress *versus* strain curve for the rate independent case. It can be observed that damage does not occur symmetrically in tension and compression, even if the corresponding strengths are equal, due to the different evolution laws used. Note also that, in the first cycle, the original undamaged stiffness is recovered upon loading reversal.

Results for Case 4 are shown in Figures 12 and 13. Figure 12 shows the stress evolution in time, compared with a purely elastic behaviour. Figure 13 shows the corresponding stress *versus* strain curve for the rate independent case. It can be observed that damage occurs only in tension, as the compressive strength is not reached. Note how the undamaged stiffness is recovered upon loading reversal.

Coupling with viscoelasticity

Two more cases are defined to study the influence of the coupling with elasticity. The values used in the models are showed in Table 3.4. Note that two different values of the retardation time for damage are used in the two cases. All units are in the SI system. Note that in both cases the ratio $f^- / f^+ = 1$, and the ratio $f_e^- / f^- = 0.5$.

Results for Case 5 are shown in Figures 14 and 15. Figure 14 shows the stress evolution in time, compared with a purely elastic behaviour. Figure 15 shows the corresponding stress *versus* strain curve for the rate independent case. It can be observed that damage does not occur symmetrically in tension and compression, even if the corresponding strengths are equal,

Variable	Case 5	Case 6
YOUNG	100 000	100 000
POISS	0.3	0.3
STREN	2 500	2 500
ILAWT	1	1
GFRAC	156.25	156.25
RETAT	0	500
RACTS	1	1
CDAMG	0.5	0.5
GFCOM	GFRAC	GFRAC
RETAC	RETAT	RETAT
NMAXW	1	1
ELAS1	0.5	0.5
RETA1	100	100

Table 3.4 Values of material properties

due to the different evolution laws used. Note also that, in the first cycle, the original undamaged stiffness is recovered upon loading reversal.

Results for Case 6 are shown in Figures 16 and 17. Figure 16 shows the stress evolution in time, compared with a purely elastic behaviour. Figure 17 shows the corresponding stress *versus* strain curve for the rate independent case. It can be observed that damage occurs only in tension, as the compressive strength is not reached. Note how the undamaged stiffness is recovered upon loading reversal.

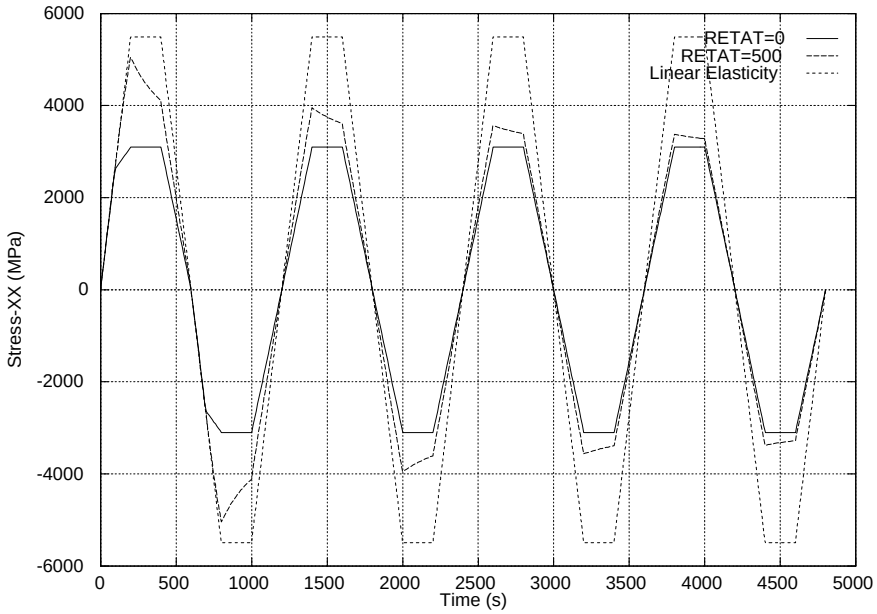

Figure 6 Stress vs. Time for Case 1

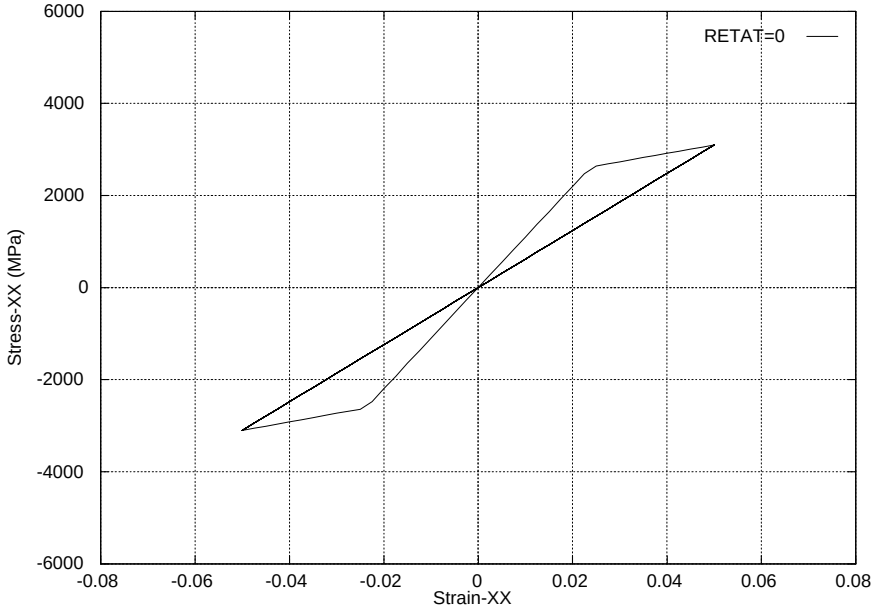

Figure 7 Stress vs. Strain for Case 1 (RETAT=0)

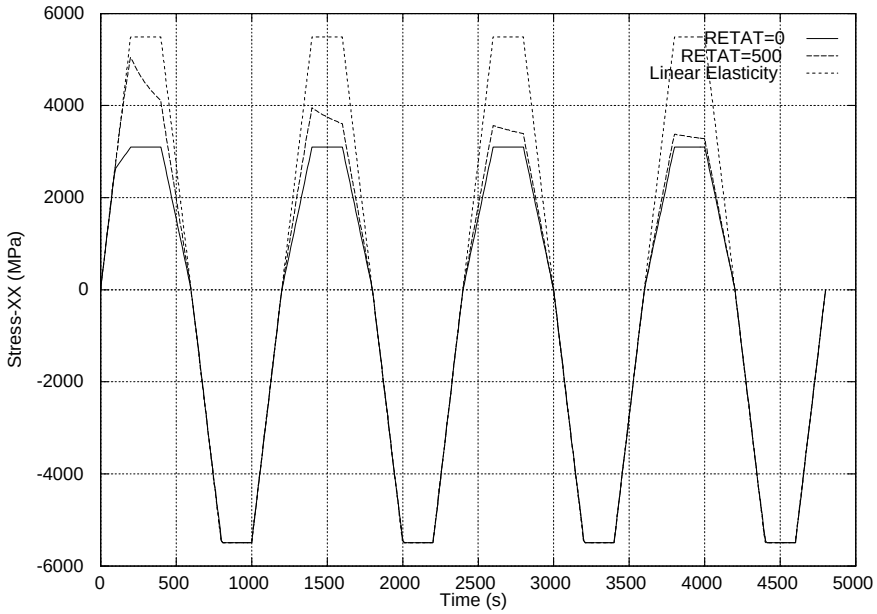

Figure 8 Stress vs. Time for Case 2

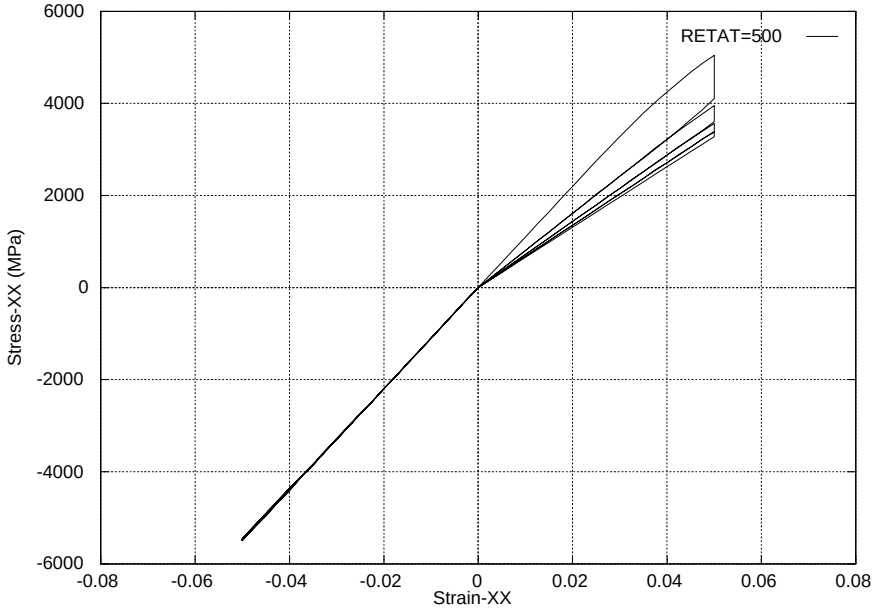

Figure 9 Stress vs. Strain for Case 2 (RETAT=500)

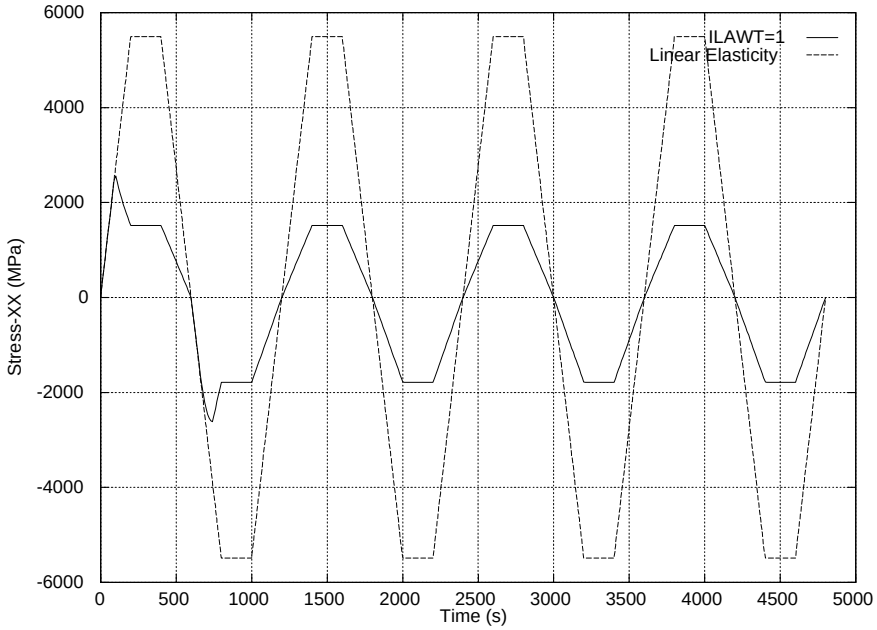

Figure 10 Stress vs. Time for Case 3

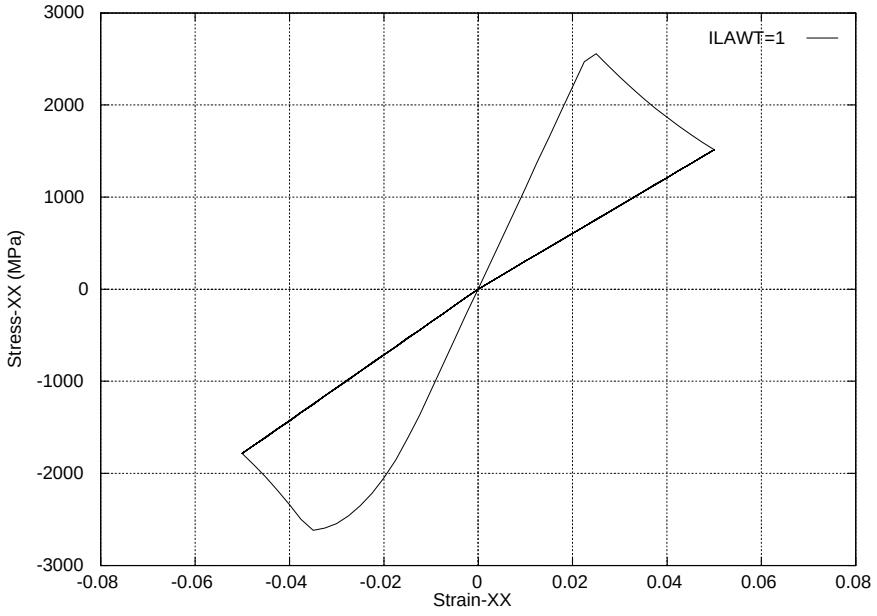

Figure 11 Stress vs. Strain for Case 3

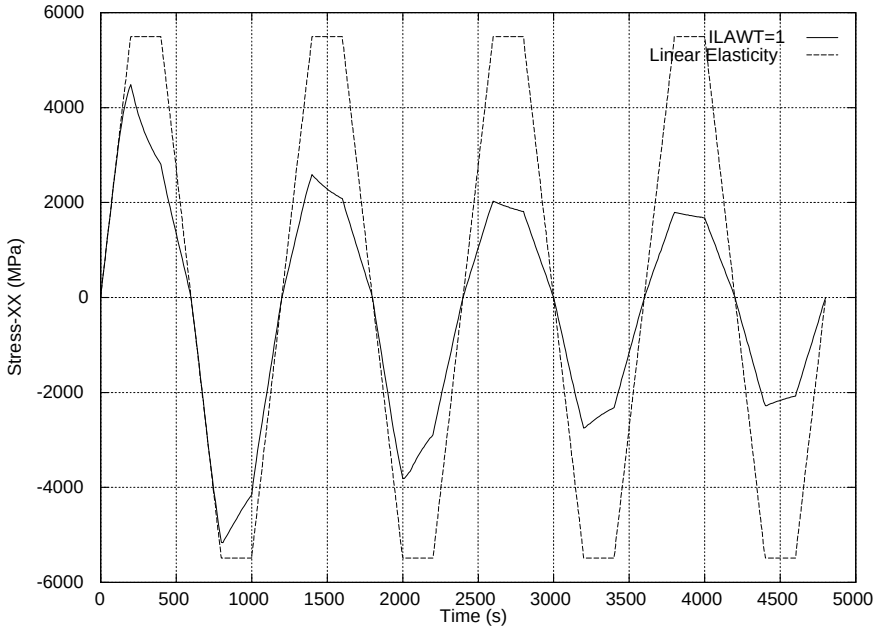

Figure 12 Stress vs. Time for Case 4

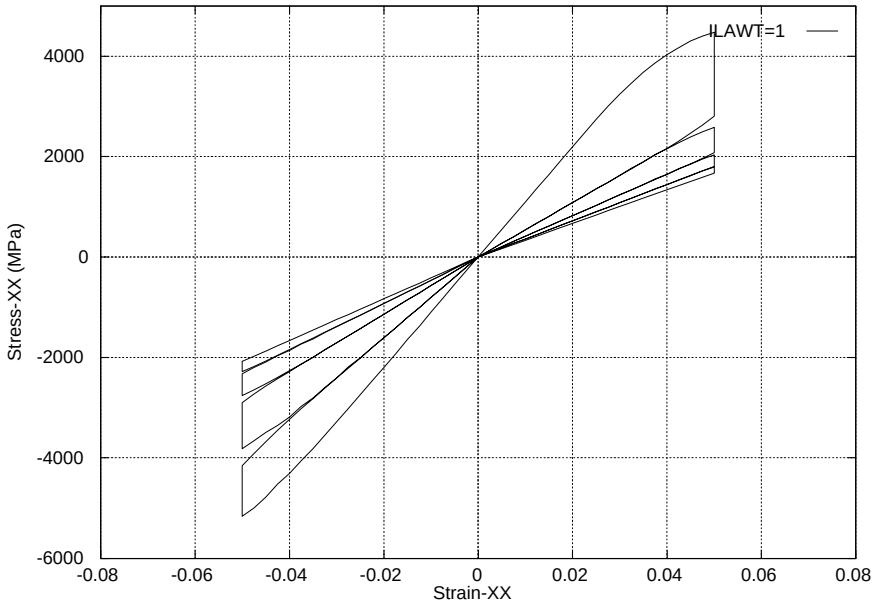

Figure 13 Stress vs. Strain for Case 4

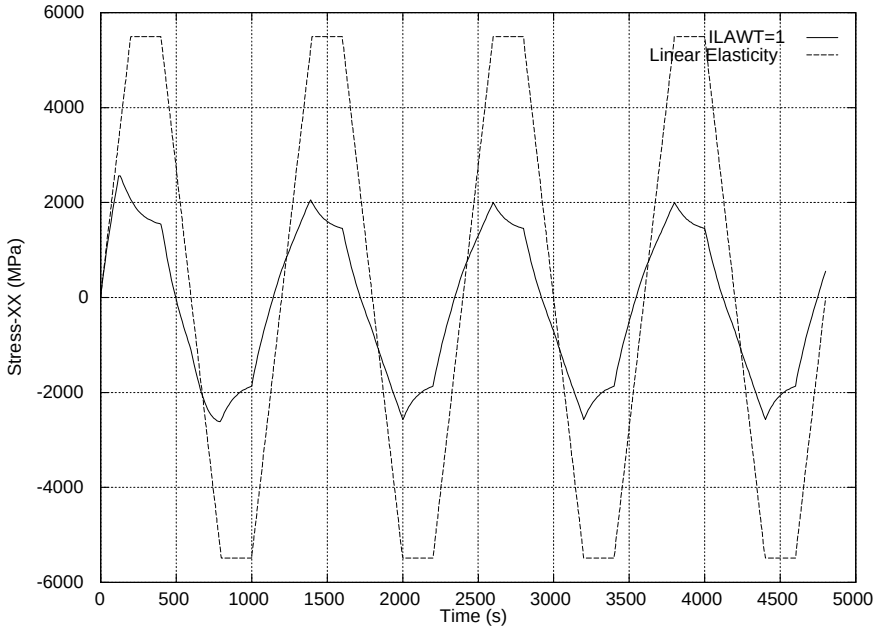

Figure 14 Stress vs. Time for Case 5

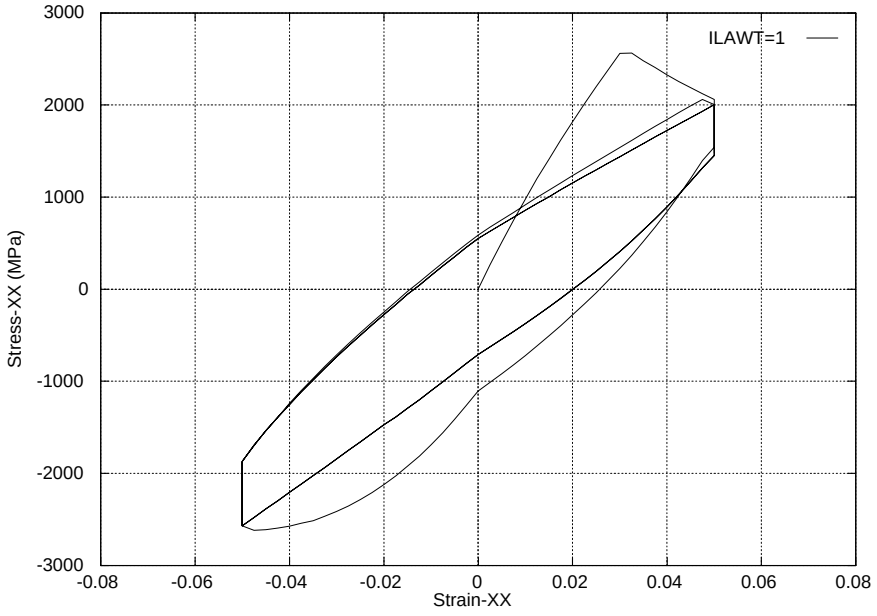

Figure 15 Stress vs. Strain for Case 5

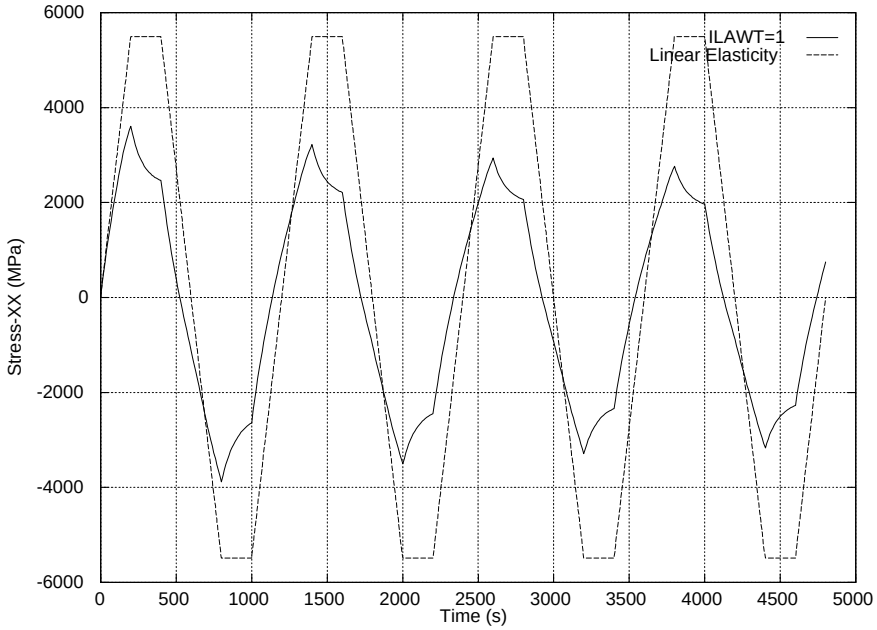

Figure 16 Stress vs. Time for Case 6

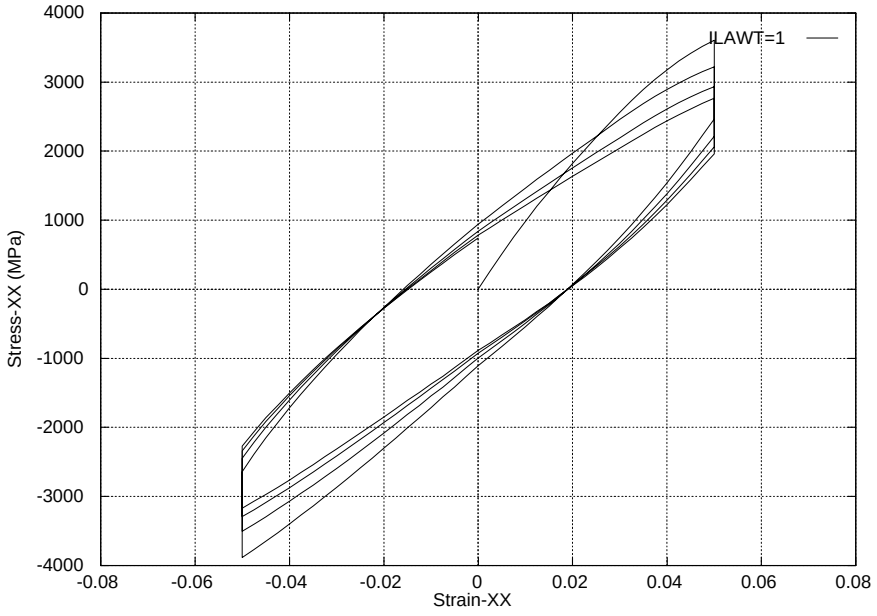

Figure 17 Stress vs. Strain for Case 6

Bibliography

[Bazant 1988] Bazant, Z. P., editor (1988). Mathematical modelling of creep and shrinkage of concrete. John Wiley & Sons, New York.

[Bicanic 1990] Bicanic, N. and Pankaj (1990). Some computational aspects of tensile strain localization modelling in concrete. Eng. Frac. Mech., 35:697–708.

[Carol and Bazant 1993] Carol, I. and Bazant, Z. P. (1993). Viscoelasticity with aging caused by solidification of nonaging constituent. J. Engrg. Mech., ASCE, 119(11):2252–2269.

[Cervera et al. 1992] Cervera, M., Oliver, J., and Galindo, M. (1992). Numerical analysis of dams with extensive cracking resulting from concrete hydration: simulation of a real case. Dam Engineering, 3(1):1–22.

[Cervera et al. 1995] Cervera, M., Oliver, J., and Faria, R. (1995). Seismic evaluation of concrete dams via continuum damage models. Earth. Engng.

Struc. Dyn., 24(9):1225–1245.

[Cervera et al. 1996] Cervera, M., Oliver, J., and Manzoli, O. (1996). A rate-dependent isotropic damage model for the seismic evaluation of concrete dams. Earth. Engng. Struc. Dyn., 25(9):987–1010.

[Cervera et al. 1998] Cervera, M., Oliver, J., and Prato, T. (1998). A thermo-chemo-mechanical model for concrete. I: Hydration and aging. J. Engrg. Mech., ASCE, 125(9):1019–1027.

[Cervera et al. 1998] Cervera, M., Oliver, J., and Prato, T. (1998). A thermo-chemo-mechanical model for concrete. II: Damage and creep. J. Engrg. Mech., ASCE, 125(9):1028–1039.

[Cervera et al. 2002] Cervera, M., Agelet de Saracibar, C. and Chiumenti, M. (2001). COMET. Coupled Mechanical and Thermal Analysis. Data Input Manual V4.0 Technical Report CIMNE, IT-308, Barcelona.

[Chaboche 1988a] Chaboche, J. L. (1988a). Continuum damage mechanics: Part I - general concepts. J. Appl. Mech., ASME, 55:59–64.

[Chaboche 1988b] Chaboche, J. L. (1988b). Continuum damage mechanics: Part II - damage

growth. J. Appl. Mech., ASME, 55:65–72.

[Faria et al. 1998] Faria, R., Oliver, J., and Cervera, M. (1998). A strain-based plastic viscous-damage model for massive concrete structures. Int. J. Solids and Structures, 35(14):1533–1558.

[Faria et al. 2001] Faria, R., Oliver, J., and Cervera, M. (2001). On isotropic damage models for the numerical analysis of concrete structures. Submitted to Int. J. Num. Meth. Engng.

[Kachanov 1958] Kachanov, L. M. (1958). Time of rupture process under creep conditions. Izvestia Akademii Nauk, Otd Tech Nauk, 8:26–31.

[Lemaitre 1984] Lemaitre, J. (1984). How to use damage mechanics. Nuclear Engineering Design, 80:233–245.

[Lemaitre and Chaboche 1978] Lemaitre, J. and Chaboche, J. L. (1978). Aspects phénoménologiques de la rupture par endommagement (in french). J. Méc. Appl., 2:317–365.

[Mazars and Pijaudier-Cabot 1989] Mazars, J. and Pijaudier-Cabot, G. (1989). Continuum damage theory: Application to concrete. J. Engrg. Mech., ASCE, 115:345–365.

[Oliver 1989] Oliver, J. (1989). A consistent characteristic length for smeared cracking models. Int. J. Num. Meth. Engng., 28:461–474.

[Oliver et al. 1992] Oliver, J., Cervera, M., Oller, S. and Lubliner, J. (1992). Isotropic damage models and smeared crack analysis of concrete. Proc. 2nd Int. Conference on Computer Aided Analysis and Design of Concrete Structures, 945–957. Pineridge Press, Swansea.

[Oliver 2000] Oliver, J. (2000). On the discrete constitutive models induced by strong discontinuity kinematics and continuum constitutive equations. Int. J. Solids and Structures, 37:7207–7229.

[Simó and Ju 1987a] Simó, J. C. and Ju, J. W. (1987a). Strain- and stress-based continuum damage models - I. formulation. Int. J. Solids and Structures, 23(7):821–840.

[Simó and Ju 1987b] Simó, J. C. and Ju, J. W. (1987b). Strain- and stress-based continuum damage models - II. computational aspects. Int. J. Solids and Structures, 23(7):841–869.